Annales Societatis Geologorum Poloniae (2023), vol. 93: 137–163 https://doi.org/10.14241/asgp.2023.07

THE STRUCTURE OF THE SILESIAN BESKID BLOCK IN THE VISTULA RIVER SOURCE AREA IN THE WESTERN OUTER CARPATHIANS (SOUTHERN POLAND)

Rafał SIKORA

Polish Geological Institute – National Research Institute, Geohazard Centre
Skrzatów Street 1, 31-560 Kraków, Poland; e-mail: rafal.sikora@pgi.gov.pl

Sikora, R., 2023. The structure of the Silesian Beskid Block in the Vistula River source area in the Western Outer Carpathians (southern Poland). *Annales Societatis Geologorum Poloniae*, 93: 137–163.

Abstract: This paper presents new results of a detailed structural analysis of the bedrock of the Vistula source area within the Silesian Beskids (Outer Western Carpathians, S Poland). The bedrock of the study area is composed of the Upper Cretaceous flysch series of the Upper Godula Beds and Lower Istebna Beds. The study area is located on the southern limb of the Szczyrk Anticline within the Silesian Beskid Block. The research is based on cartographic field work and remote sensing analysis of a digital elevation model from LiDAR data. The structural analyses were supported by the extraction of the topolineaments and their spatial analysis. The results presented show that the monoclinal bedrock structure of the study area can be characterized by a systematic joint pattern, which determined the existence of faults and fault zones. Moreover, detailed analyses show differences in fracturing of the sedimentary strata and the existence of hidden fracture zones, not visible in the previous map view. Most of the faults are related to an orthogonal joint system, whereas the transverse and longitudinal faults are connected with fold and thrust structures that are exposed in outcrops and reflected in the topography. Kinematic analysis shows that the NW–SE-trending transverse faults underwent dextral movements, while the ENE–WSW-trending longitudinal faults recorded sinistral displacements. Furthermore, older strike-slip and oblique-slip displacements along faults were overprinted by normal dip-slip faulting. The new tectonic and relief data show no existence of the Gościejów Syncline in the northern part of the study area, which was depicted on previous maps. In conclusion, normal faulting and damage of the bedrock along fracture zones are interpreted as being related to the post-tectonic, gravitational collapse of the rock massif. Its detailed recognition is very important for the further study of relationships between bedrock structure and mass movement characteristics, such as the geometry and kinematics of landslides.

Key words: Lineaments, hidden fracture zone, structural analysis, Szczyrk Anticline, Silesian Beskid Block, Outer Carpathians.

Manuscript received 25 April 2022, accepted 14 June 2022

INTRODUCTION

The bedrock structure in the Silesian Beskids of the Western Outer Carpathians (Oszczypko *et al*., 2008; Solon *et al*., 2018; Figs 1, 2) have not received much attention in the past. So far, studies were concentrated mainly on sedimentary facies and stratigraphic issues (Szajnocha, 1923; Unrug, 1963; Geroch and Nowak, 1980; Słomka, 1995; Strzeboński, 2022). The first studies on the tectonics of this area were carried out at the beginning of the 20th century (Nowak, 1927) and continued in the 1930s (Burtanówna *et al*., 1937). The general outline of the bedrock structure was drawn by Książkiewicz (1953), who distinguished individual blocks within the Silesian Nappe. Further tectonic studies approximated general structural trends in relation to the other parts of the Polish Outer Carpathians (Książkiewicz, 1968; Mastella and Konon, 2001, 2002; Tomaszczyk, 2005). The most nearly complete structural interpretation was developed in the 1970s and at the turn of the 20th and 21st centuries and was based on the Skoczów, Bielsko-Biała, Milówka and Vistula Sheets of the Detailed Geological Map of Poland (DGMP; Burtan, 1973; Nescieruk and Wójcik, 2012, 2013a, b, 2014, 2016, 2017; Ryłko, 2018, 2019).

The present study covered an area of 61 km^2, situated in the Vistula River source area on the western slopes of the Barania Góra Range in the southern part of the Silesian Beskids, geologically corresponding to the southern part of the Silesian Beskid Block (Fig. 2A). The objective of the study was to elaborate in detail the structural features of the Silesian Beskid Block in the Vistula River source

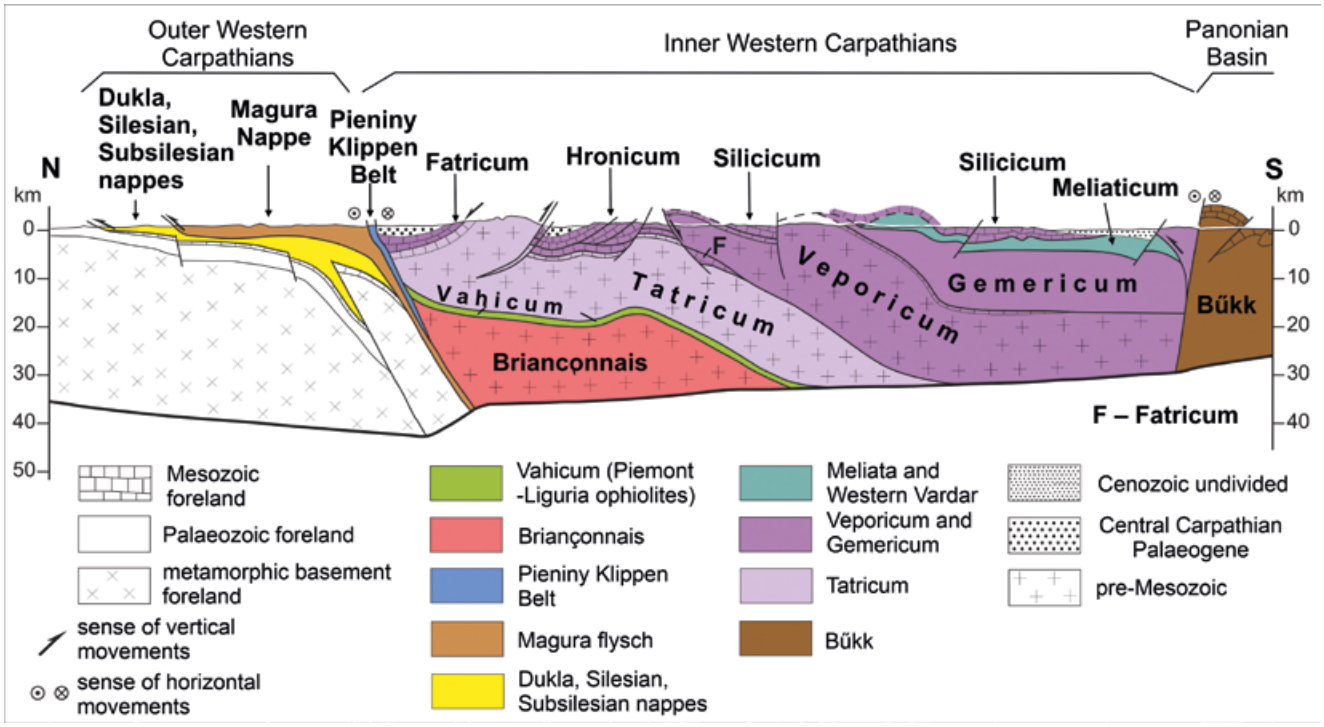

Fig. 1. Position of the Outer Western Carpathian nappes with respect to the units of the ALCAPA block and the European foreland (modified after Schmid *et al*., 2020).

area (Barania Góra Range), where only a few dislocations had been reported previously (Burtan, 1972; Neścieruk and Wójcik, 2016, 2017). On the other hand, numerous rocky landslides have developed in this area, sometimes of considerable size, and landslide groups occupying entire mountain slopes (Sikora and Piotrowski, 2013a, b). Detailed field and laboratory studies on joints and faults of the study area can be useful for the recognition of nature of the bedrock structure and an understanding of the relationships between the post-orogenic relaxation of the rock massif and mass movement. Preliminary studies have demonstrated a relationship between faults and fracture zones and the development of landslides (Sikora, 2017, 2018).

Nowadays, the correct recognition of the bedrock structure in the Silesian Beskids is important for the analysis of passive factors responsible for landslide development (Bober, 1984; Wójcik, 1997; Margielewski, 2002, 2006; Pánek *et al*., 2010, 2011) and for geotechnical and engineering activities. The latter are connected with the expansion of communication infrastructure and the construction of new housing estates. From such a perspective, the mapping of bedrock structure on a 1:50,000 scale of the DGMP does not reflect its proper nature and for the purposes mentioned above is too general. According to the Landslide Counteracting System in Poland (SOPO), the registration of landslides in this area is carried out on the 1:10,000 scale (Grabowski *et al*., 2008) and engineering works require even more detailed data. Another practical application of the results can be an understanding of the structural anisotropy of the rocks series that is useful for fractured reservoir modelling and prediction of the fracture corridors in the rock massif (Watkins *et al*., 2018).

REGIONAL GEOLOGY AND TECTONIC SETTINGS

The Outer Carpathian orogenic wedge was formed as a result of the closure of the Alpine-Tethys (Balla, 1987) during the Late Cretaceous (Żytko, 1999; Oszczypko *et al*., 2008; Golonka *et al*., 2019). The Western Outer Carpathians domain is an asymmetric fold and thrust belt, which was formed in the Oligocene–Miocene as a result of the collision of the ALCAPA (Alpine-Carpathian-Pannonian) and Tisza-Dácia blocks (mega-units) with the European Platform (Unrug, 1980; Pescatore and Ślączka, 1984; Rauch, 2013, 2015; Kováč *et al*., 2016, 2017; Schmid *et al*., 2020; Fig. 1). In the territory of Poland, they stretch in a wide arc from SW to SE (from the borders with the Czech Republic and Slovakia to the border with Ukraine; Fig. 2A, B). The Polish part of the Western Outer Carpathian prism is divided into several nappes: the Magura Nappe, the Dukla Nappe and the Fore-Magura Nappe, the Silesian Nappe, the Sub-Silesian Nappe and the Skole Nappe (Żytko *et al*., 1988; Oszczypko *et al*., 2008; Fig. 2B). The Silesian Nappe is the second largest of them and in the western part it is subdivided into the Beskid Jabłonkowski Block, the Silesian Beskid Block and the Beskid Mały Block as a result of the disharmonic folding. Their boundaries are the NW–SE tear faults, running transversely to the regional fold and thrust structures (Książkiewicz, 1953, 1972). Tear faults and numerous joint sets were formed during the final phase of fold and thrust deformation (Tokarski, 1975; Aleksandrowski, 1985; Tokarski *et al*., 1999; Rubinkiewicz, 2000, 2007; Mastella and Konon, 2001, 2002; Barmuta *et al*., 2021). The structure of the Polish Outer Carpathians was subject to strong overprint after the cessation of Alpine folding. There was the development of

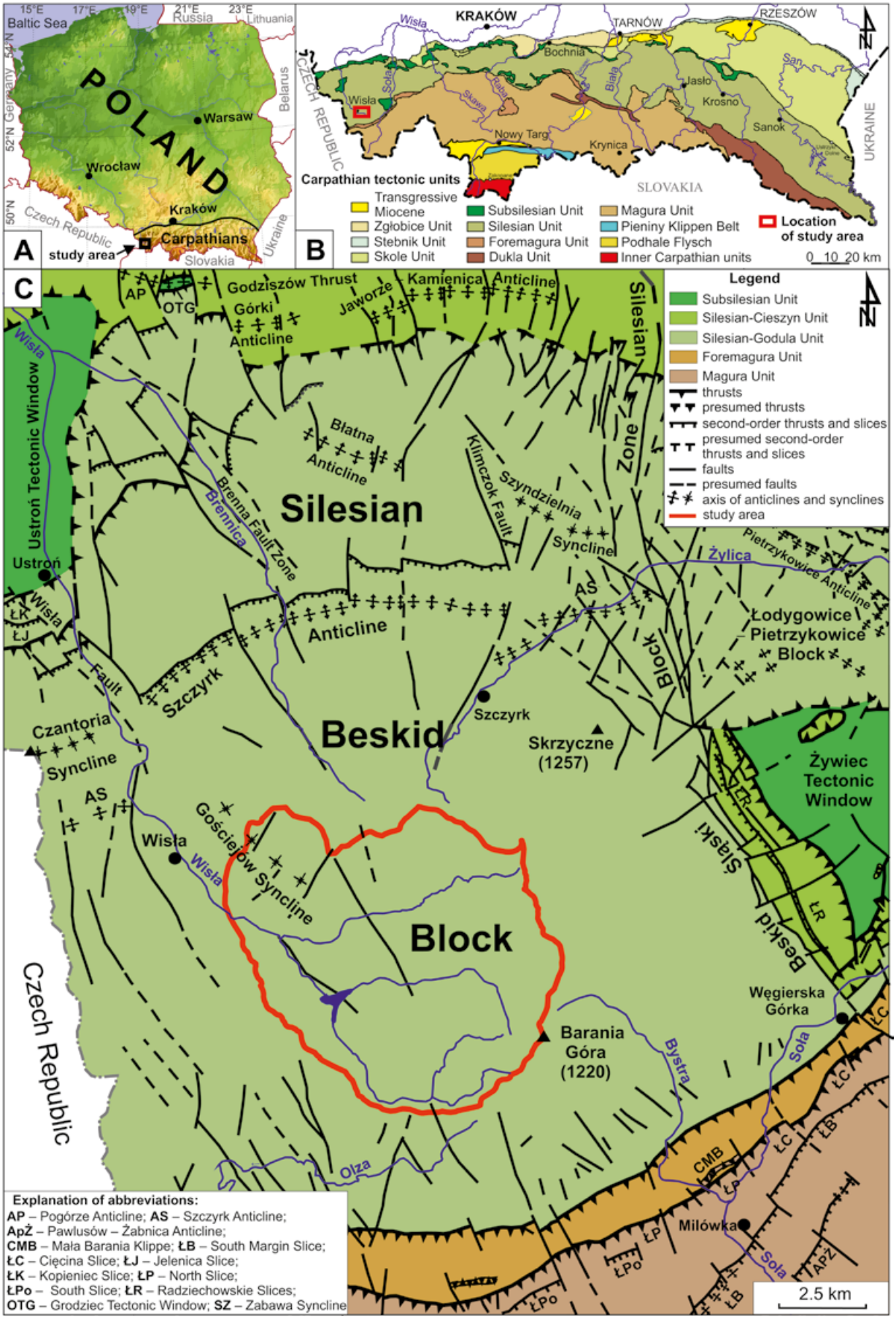

Fig. 2. Location of the study area. **A.** On the territory of Poland. **B.** In the Polish segment of the Western Carpathians. **C.** Study area outlined in red on a structural map of the Silesian Beskid Block and adjacent areas (after Burtan, 1973; Żytko *et al*., 1988; Nescieruk and Wójcik, 2012, 2013a, b, 2014, 2016, 2017; Ryłko, 2019).

numerous normal faults, which were related to the post-orogenic tectonic relaxation of the rock massif (Zuchiewicz, 1997, 1999, 2001; Zuchiewicz *et al*., 2002; Andreucci *et al*., 2013; Jankowski and Margielewski, 2014, 2022).

The Silesian Beskid Block (SBB; Książkiewicz, 1953, 1972) comprises the Godula Sub-nappe (upper, the Silesian-Godula Sub-nappe) thrust over the Cieszyn Sub-nappe (lower, the Silesian-Cieszyn Sub-nappe; Nowak, 1927; Paul *et al*., 1996). The northern boundary of the SBB is emphasised by a distinct, structural ridge, developed along the overthrusts on the Subsilesian Nappe, whereas its southern fragment is hidden under the Fore-Magura and the Magura thrusts (Fig. 2C). The cartographic data available show that fold structures, overthrusts and transverse faults occur mainly in the northern and southern parts of the SBB (Burtan, 1972; Neścieruk and Wójcik, 2017; Ryłko, 2019; Fig. 2C). The eastern edge of the SBB is the NNW–SSE-striking Silesian Beskid Fault Zone (SBFZ; Paul *et al*., 1996). It is a complex system of faults and overthrusts (middle–late Miocene age; Decker *et al*., 1997; Neścieruk, 2001), separating the SBB from the Beskid Mały Block (BMB, in the north) and the Żywiec Tectonic Window (ZTW, in the south). The SBFZ is generally a scissors fault, along which the northern part of the SBB is elevated and the southern part is lowered (Książkiewicz, 1972). The western part of the SBB is located in the Czech Republic, where it is separated by a set of thrusts and dislocations from the Beskid Jabłonowski Block (BJB; Książkiewicz, 1972; Paul *et al*., 1996).

The SBB shows features of a south-dipping monocline (Książkiewicz, 1953, 1972). Within its area, there are second-order tectonic structures: thrusts, thrust slices and folds, mainly with ENE–WSW trends and subordinately with WNW–ESE trends (Burtanówna *et al*., 1937; Neścieruk, 2001; Neścieruk and Wójcik, 2012, 2013b, 2016, 2017). The geometry of the folds is related to the competence of rocks: the folds in thick-bedded formations (conglomerates and sandstones) are cylindrical, symmetrical and open. In thin-bedded formations (shales and sandstones), the folds are tight and asymmetrical. The southern limbs of the folds are long and sliced (Neścieruk, 2001). In the central part of the SBB, the ENE–WSW trending Szczyrk Anticline is most clearly marked (Fig. 2C). The southern flank of the Szczyrk Anticline is flat and extends over several kilometres.

On the basis of the cartographic data (Neścieruk and Wójcik, 2017; Ryłko, 2018, 2019), the weakly folded or flat bedrock in the central part of the Silesian Beskids is almost devoid of faults (Fig. 2C). This indicates that to date there is very limited structural information available from the bedrock in this area.

STRATIGRAPHY

The Godula Sub-nappe flysch succession comprises formations from Lower Cretaceous to Palaeogene with thicknesses of up to 5,000 m. The lower part of its profile is composed of the strongly tectonically modified Veřovice Beds (Hauterivian), the trigeminal sequence of the Lgota Beds (Albian–Cenomanian) and the trigeminal succession of the Godula Beds (Santonian–Campanian; Fig. 3). The middle part comprises the two levels of the Istebna Beds (Maastrichtian–Paleocene). In upper part of the profile, the variegated shales, the Ciężkowice Sandstones (Paleocene–Eocene), the Hieroglyphic Beds (Eocene), the Globigerina Marls (Eocene), the Menilite Beds (Oligocene) and the Krosno Beds (Oligocene) were distinguished (Burtan, 1973; Geroch and Nowak, 1980; Ryłko and Żytko, 1980; Paul *et al*., 1996). In terms of lateral extent and thickness, the most important lithostratigraphic units in the Godula Sub-nappe are the Godula Beds and the Istebna Beds (Figs 2C, 3). They constitute the main body of the unit discussed. The Godula Beds occur in the axial zone and the northern limb of the Szczyrk Anticline. The southern limb of the anticline mainly consists of the Godula Beds and the Istebna Beds, and its southernmost part, the Ciężkowice Sandstones, the Hieroglyphic Beds, the Melinite Beds, and the Krosno Beds (Paul *et al*., 1996).

In the northern part of the study area, the Upper Godula Beds (UGB; Santonian–Campanian; Słomka, 1995; Golonka and Krobicki, 2017) are the main component. It is a complex (500 m thick) of thin- to medium-bedded, massive, fine-grained sandstones with parallel laminations, which have interbeds of grey or greenish mudstones, up to 40 cm in thickness (Fig. 4; Burtan, 1973; Neścieruk and Wójcik, 2017). The Malinowska Skała Conglomerate occurs locally, in the roof of the UGB (Fig. 2; Burtanówna *et al*., 1937; Burtan *et al*., 1959; Burtan, 1972, 1973; Neścieruk and Wójcik, 2017; Ryłko, 2018). These are thick-bedded conglomerates and sandstones reaching a thickness of 50 m and in the stratotype profile even as much as 120 m (Burtan, 1973). They are characterised by thin interbedding (up to 8 cm) of mudstones with plant detritus and the occurrence of exotics, comprising pebbles of gneiss, granite, and sedimentary rocks (Burtan, 1972; Neścieruk and Wójcik, 2016). Outcrops of the Malinowska Skała Conglomerate are situated in the upper parts of the Barania Góra Range, in the eastern part of the study area (Fig. 4). A smaller occurrence of these rocks is located in the north-western part of the Cienków Ridge, at the confluence of the Wisełka and the Malinka valleys (Burtan, 1972; Neścieruk and Wójcik, 2017; Ryłko, 2018).

The Lower Istebna Beds (LIB; Campanian–Maastrichtian; Burtanówna *et al*., 1937; Unrug, 1963; Neścieruk and Szydło, 2003) lie above the UGB. The LIB occur mainly in the southern part of the study area. In addition, an outlier of them is located in the north-western part, in the Gościejów Valley. The sedimentary transition between the two lithostratigraphic units is gradual (Burtan, 1973; Strzeboński, 2022) and is exposed in the Biała Wisełka Valley (Burtan, 1972; Neścieruk and Wójcik, 2017; Fig. 4).

The LIB are mainly thick-bedded sandstones and conglomerates, with individual beds reaching a thickness of 4.5 m, and the thickness of the entire profile reaches 400 m (Fig. 3). The mineral composition of the sandstones is dominated by quartz and feldspar, with muscovite occurring subordinately. The conglomerates contain pebbles of granite, gneiss, schists, and limestone. In the bottom and top intervals of the LIB, among the conglomerates, there are

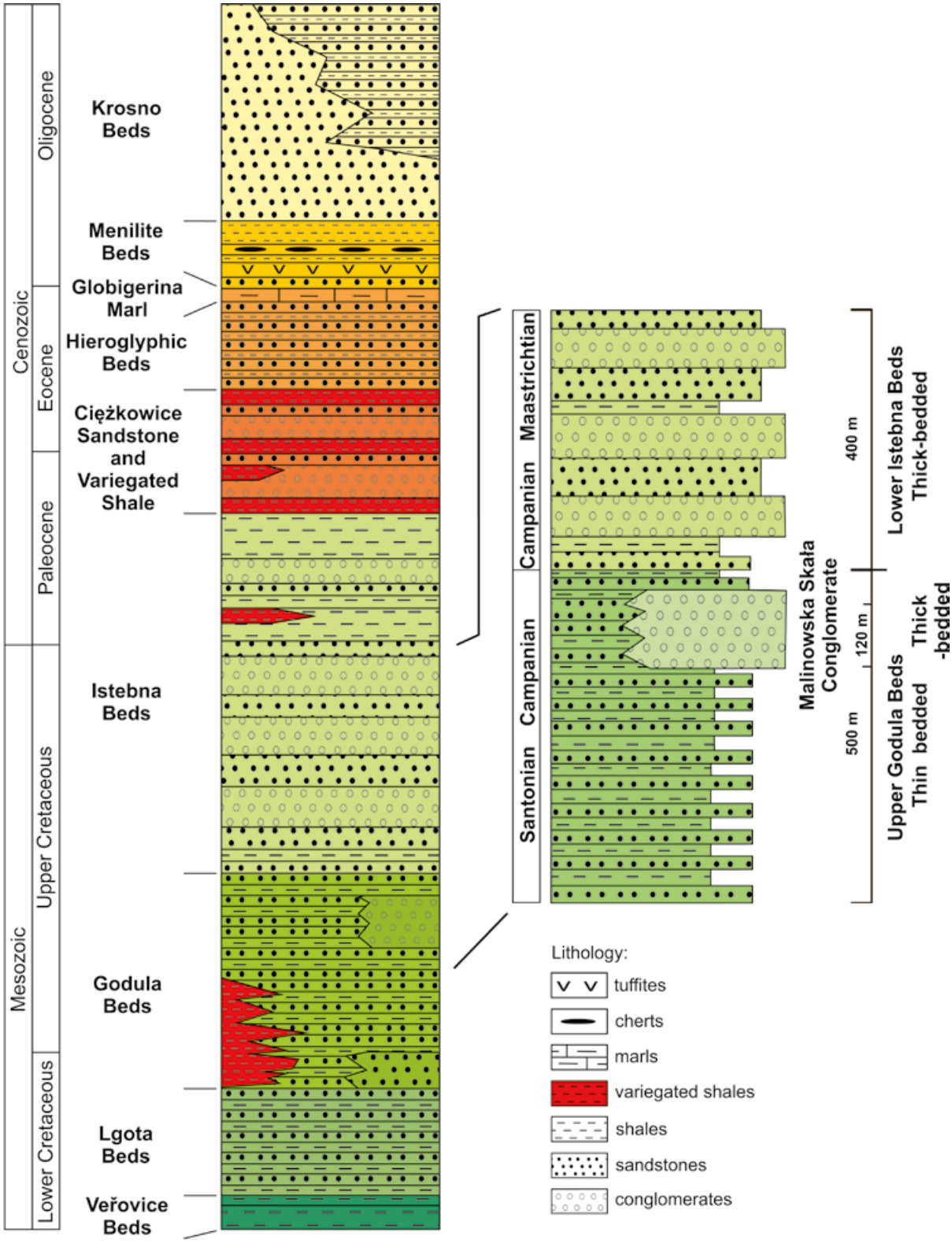

Fig. 3. Synthetic lithostratigraphic profile of the study area compared with the lithostratigraphic series of the Godula Sub-nappe (after Cieszkowski *et al*., 2009, modified).

intercalations of mudstone with plant detritus and lenses of mudstone up to 12 m thick, with exotic clasts.

The flysch rocks are covered with Quaternary colluvial material, rock rubble, and weathered clays, with detrital fragments of bedrock (Burtan, 1973; Sikora and Piotrowski, 2013a; Neścieruk and Wójcik, 2017).

STRUCTURE OF THE BEDROCK OF THE STUDY AREA

The study area comprises the central part of the southern limb of the NW–SE-trending Szczyrk Anticline with the Gościejów Syncline occurring subordinately. In the axial

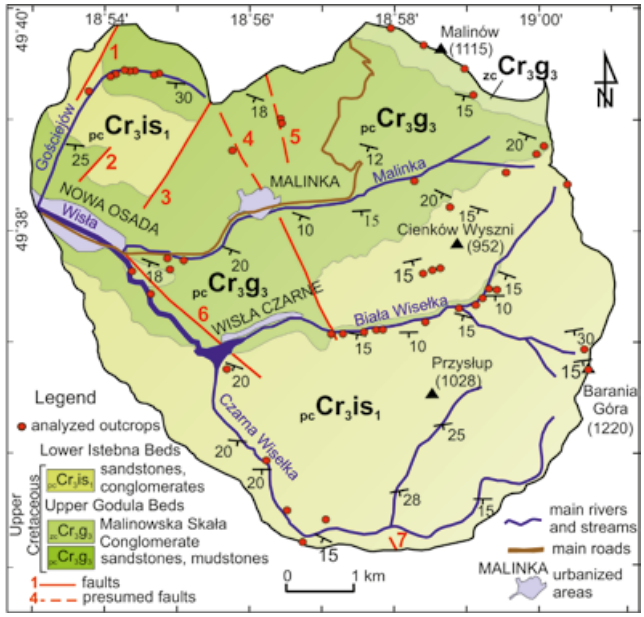

Fig. 4. Geological map of the study area without Quaternary deposits (modified after Burtan, 1972; Neścieruk and Wójcik, 2017).

zone of the Gościejów Syncline are the LIB rocks (Fig. 2C; Burtan, 1972; Neścieruk and Wójcik, 2016, 2017).

The geological maps of the area do not show the trends of the overthrusts (Figs 2C, 4; Burtan, 1972; Neścieruk and Wójcik, 2017) and show only incomplete recognition of the disjunctive tectonics of the bedrock. Seven faults were marked in the area (Fig. 4; Burtan, 1972; Neścieruk and Wójcik, 2017). Four of them, with NW–SE and NNW–SSE trends, coincide with the orientation of most of the dislocations found in other parts of the SBB and are partly masked by landslide colluviums (Neścieruk and Wójcik, 2012, 2013b, 2017; Ryłko, 2018). The longest fault (No. 4), marked in the central part of the area, strikes NW–SE from the Równica Ridge through the Cienków Ridge to the Biała Wisełka Valley (Fig. 4). Its southern section separates the LIB outcrops on the eastern flank from the UGB on the western flank. The remaining 3 faults, marked on geological maps of the study area, strike in a NE–SW direction and are situated in the upper part of the Smrekowiec Mountain (982 m a.s.l.) and on the slopes of the Gościejów Valley (Fig. 3; Burtan, 1972; Neścieruk and Wójcik, 2017). These faults limit and displace outcrops of the LIB in relation to the UGB.

The systems of joints and their orientations, relative to the strike of regional fold structures and to the thickness of rocks in the flysch series of the Polish Carpathians, were described by Boretti-Onyszkiewicz (1968) and Książkiewicz (1968). These descriptions were expanded and detailed in later years by Mastella (1972), Tokarski (1975), and Aleksandrowski (1985, 1989). The nature of the joints in the Polish Outer Carpathians was also studied by Mastella (1988), Zuchiewicz and Henkiel (1993), Mastella *et al.* (1997), Zuchiewicz (1997, 1999), Rubinkiewicz (1998), Tokarski *et al.* (1999), Mastella and Zuchiewicz (2000), Konon (2001), Mastella and Konon (2001, 2002) and Neścieruk (2001).

Five main joint sets were distinguished by Książkiewicz (1968) and Mastella and Konon (2001) in the study area. Their classification is based on their orientation, relative to the axis of regional folds (Fig. 5; Tab. 1). Two sets of joints represent a shear system, referred to as S_R (formed by dextral shear) and S_L (formed by sinistral shear), with directions 100–117° and 164–182°, respectively. These shear fractures form a conjugate system, which is diagonal to the strike of fold axis. The remaining joints are longitudinal (parallel to fold axis) joints L with direction 50–63°, longitudinal oblique (low angle to the fold axis) joints L' with direction 67–85°, and transverse (perpendicular to the fold axis) joints T with direction 140–151°. Moreover, in the area of the Godula Nappe, Tomaszczyk (2005) additionally distinguished a sixth, low-angle set, L", with a direction of 20–38° (Fig. 5; Tab.1). This is probably the same set as the joints with a direction of 10°, identified by Mastella and Konon (2001). According to Margielewski *et al.* (2008), the diagonal joint sets D1 (S_R in this paper) and D2 (S_L in this paper) strike in directions 130–140° and 220–240°, respectively, the L set 260–280°, and the T set 340° (Tab. 1).

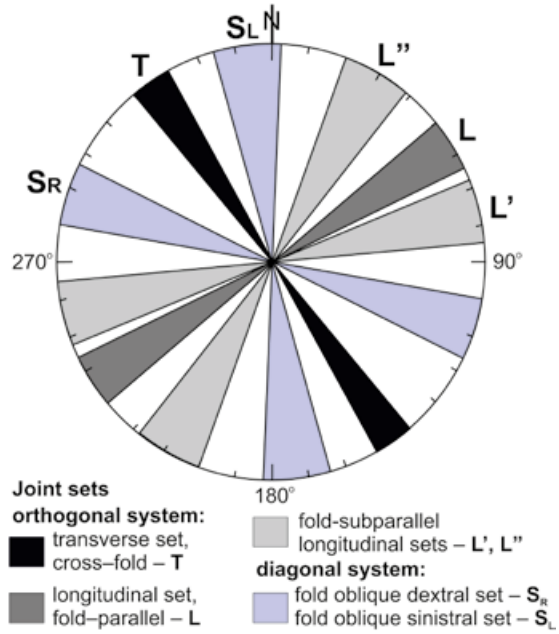

Fig. 5. Orientation of the joint sets and systems distinguished in the western part of the Silesian Nappe (after Książkiewicz, 1968; Mastella and Konon, 2001; Tomaszczyk, 2005).

Table 1

Trends of the joint sets of the Silesian Nappe in the Wisła area.

Joint sets	after Mastella and Konon (2001)	after Tomaszczyk (2005)	after Margielewski *et al.* (2008)
S_R	90–114°	100–117°	130–140°
S_L	155–169°	164–182°	40–60°
T	140 °	140–151°	160°
L	60 °	50–63°	80–100°
L'	90°	67–85°	–
L"	10°	20–38°	–

METHODS

Fieldwork

The research was based mainly on fieldwork and numerical terrain-model analysis. The field structural studies included observations and measurements of the orientation of planar (bedding planes, joints, and faults) and linear (striations) structures. During the research, attention was paid to the morphology of the observed fracture surfaces and the presence of small, tectonic structures (steps, feather fractures, drag folds, axial cleavage, horsetail splays, etc.), indicating the kinematics of fault displacements (Hanckok, 1985; Aleksandrowski, 1992; Dadlez and Jaroszewski, 1994; Żaba, 1999). The study area is characterised by a high degree of landslide occurrence (Sikora, 2018), so special attention was paid to the fact that the measurements were made in outcrops, situated outside the landslides.

The joints were analysed separately for each lithostratigraphic section. The density of joints depends on the thickness of layers (Boretti-Onyszkiewicz, 1968; Mastella, 1972) and, thus, the greatest number of measurements was collected in outcrops of the thin-bedded UGB. On the other hand, attention was drawn to local dense fractures within the thick-bedded sandstones and conglomerates of the LIB and the Malinowska Skała Conglomerate, which may indicate the occurrence of tectonic disturbance zones (Mastella, 1972; Hennings *et al*., 2000).

While recording the fractures, attention was paid to the nature of their surfaces, i.e., dilatation, presence of mineralisation, and occurrence of small-scale, tectonic structures (Aleksandrowski, 1989; Will and Wilson, 1989; Dunne and Hanckock, 1994; Zuchiewicz, 1997; Rybak, 2006; Davis *et al*., 2011). The identification of individual sets of joints was based on their characteristic morphological features, indicated by Książkiewicz (1968), Tokarski (1975), Aleksandrowski (1989), Mastella and Konon (2001, 2002), Tomaszczyk (2005), and Ludwiniak (2008).

Structural plotting

The data on the spatial orientation of planar structures (bedding planes, joints, and faults) in individual outcrops and the relationship to lithostratigraphic sections were subjected to geometrical, kinematic, and statistical analyses (Turner and Weiss, 1963; Ramsay, 1967; Teisseyre, 1971; Jaroszewski, 1972, 1980; Ragan, 1973; Liszkowski and Stochlak, 1976; Ramsay and Huber, 1987; Aleksandrowski, 1992; Mierzejewski, 1992; Żaba; 1999). Geometrical projections of tectonic structures were made on the lower hemisphere of the Lambert-Schmidt equal-area net Circular plots, contour diagrams, rosette diagrams, and histograms were used to represent statistically and analyse the results. Fabric8 (Wallbrecher, 1986), Orient (Vollmer, 2015), and MS Excel 2010 software were used for this purpose. The starting point of the structural analysis was to determine the arrangement of strata orientation in the study area, which may indicate the presence of tectonic structures (primarily folds and faults). To analyse in detail the orientation of strata in the study area, the data contained in the DGMP (Neścieruk and Wójcik, 2017) were compiled with the present author's own measurements. Rosette diagrams were used to determine the directions of joint sets in individual outcrops and for each lithostratigraphic unit. They were plotted in classes of 10 degrees. In the kinematic analysis, minor structures that indicate the sense of relative movement: slickenlines, tectonic steps, and geometrical arrangement of fractures according to the Riedel-Skempton model (Riedel, 1929; Skempton, 1966) were used.

Topolineament extraction on LiDAR-based elevation model

An indirect method for the determination of faults in the study area was the analysis of lineaments, based on the interpretation of a three-dimensional Digital Elevation Model (DEM) with a 1x1 m resolution, acquired using airborne laser scanning, the LiDAR (Light Detection and Ranging) method. The LiDAR-DEM model was obtained from the resources of the Head Office of Geodesy and Cartography (GUGiK). Global Mapper, ILWIS, and ArcGIS software were used for the analysis with proper visualisation of the model (Wojciechowski, 2009; Ozimkowski, 2010; Scheiber *et al*., 2015).

The concept of lineaments for geological studies was introduced by Hobbs (1904, 1912). A lineament is defined as a linear feature of the land surface or its composition, which may reflect some phenomena in the subsurface (O'Leary *et al*., 1976). The definition of photolineaments and their role in bedrock analysis were undertaken by Bażyński and Graniczny (1978), Ostaficzuk (1981) and Dadlez and Jaroszewski (1994). The application of the analysis of lineaments is based on the assumption that they reflect the effects of mechanical processes within the bedrock and indicate discontinuous structures in the rock (Graniczny and Mizerski, 2003). Moreover, their density may be a result of young tectonic uplift, which caused the gravitational rejuvenation of discontinuous surfaces (Jaroszewski and Piątkowska, 1988).

In the research presented below, topolineaments, i.e., rectilinear features of the relief with high repeatability of directions, were analysed (Badura and Przybylski, 2005). The topolineaments were determined manually which allowed exclusion from the analysis of features connected with infrastructure (roads, railways, etc.; Koike *et al*., 1995; Mah *et al*., 1995; Suzen and Toprak, 1998; Koçal *et al*., 2004; Scheiber *et al*., 2015). The direction and length of the topolineaments were analysed and presented on diagrams and histograms. The spatial distribution of linear elements was used to develop a map of their density (in the Global Mapper software). Linear objects were transformed into a point cloud, then a density map was plotted according to the Gaussian Kernel distribution (distance weighted at 100 m radius, 5 samples per radius). Analysis of the orientation, occurrence and density of topolineaments allowed establishment of their relationship with the observed joint sets, and helped to determine the strikes of delineated faults. The determination of faults based on topolineaments took into account their relationship with the extension of morphological ridges and fissures on slopes and changes in the trends of rock outcrops that were visible on the terrain model. As a rule, many faults delineated in this way were marked as presumed.

RESULTS

Bedding planes orientation

The analysis of strata orientation was based on measurements from 221 locations in the study area. The rock layers most often plunged to the SW and SSW, less frequently to the S, and occasionally to the W and SE. The dip angles of the strata ranged from 15 to 28° (Fig. 6). Locally, the strata also dip towards the W and SE and the dip angles exceeded 35°. The orientation of bedding planes is frequently differentiated, owing to local rotation caused by nearby landslide processes and the occurrence of faults. Changes in strata orientation often result from uneven stratigraphic surfaces. The contour diagram of the orientation of bedding planes (Fig. 6A) clearly shows a monoclinal arrangement in the study area. This is indicated by a strongly concentrated maximum of the measurements.

Joints

The analyses of joints were based on observations in 43 outcrops, in which 2,690 measurements were made (Fig. 4). The diagrams show the dispersed distribution of joints in the studied area, among which privileged strikes can be distinguished (Fig. 7A–C). The greatest number of fractures (1,457) was measured in the thin-bedded lithotypes of the UGB and much less in the thick-formed Malinowska Skała Conglomerate (334) and the LIB sandstones and conglomerates (899). The joints are generally steep, with dip angles ranging from 75 to 90°; there are far fewer joints dipping at angles between 60–75° and 45–60°, and very few joints with a dip angle of less than 45°. Joints with dip angles below 30° were not recorded in the LIB. The prevalence of steep joints in the monoclinal, layered system with dip angles of 5–25° indicates the predominance of kathetal joints in the rock massif (Fig. 7D–F). Some dependence of the joint pattern on the lithostratigraphic series was noticeable (Fig. 7). On the basis of the joints analysis, it can be concluded that there are zones characterised by a constant arrangement of fractures in the study area: a northern area with a distribution typical of the UGB; a central area - mixed, where the UGB are covered by the LIB; and a southern area with a joint arrangement characteristic for the LIB.

Within the thin-bedded UGB, the joint sets of an orthogonal system are the most prominent (Fig. 7A). In particular, the T set strikes NW–SE (320+/-10°) and the longitudinal set (L) NE–SW (55+/-5°). The other sets are less pronounced: L' joints strike 85–90°, and L" joints strike within a range of 10 to 28° (Fig. 7A). Weaker but pronounced are also the joint sets of the diagonal system, which strike at 290° in the case of the S_R set The joints of the S_L set do not form a distinctive maximum.

Less dispersion of joint directions occurs within the Malinowska Skała Conglomerate (Fig. 7B). The most prominent joints in these rocks are those of the L set, following the same direction as in the UGB thin-bedded sandstones and mudstones (55+/-5°). The L" joints are slightly less pronounced in these rocks (24+/-5°). The T-type joints show a more pronounced dispersion than that in the thin-bedded series. Their maxima strike to 315°, 325° and 340°. In the Malinowska Skała Conglomerate, the L' type joints are very weak and strike at 80°. The presence of joints of the diagonal system was rarely recorded in these conglomerates. Only the S_R set (285°) is marked on the diagram (Fig. 7B).

The LIB is dominated by the L' and L joint sets of the orthogonal system (Fig. 7C). Książkiewicz (1968) believed that longitudinal joint set was missing in places. These joint sets reveal orientations of 70+/-5° and 55+/-5°. A significant

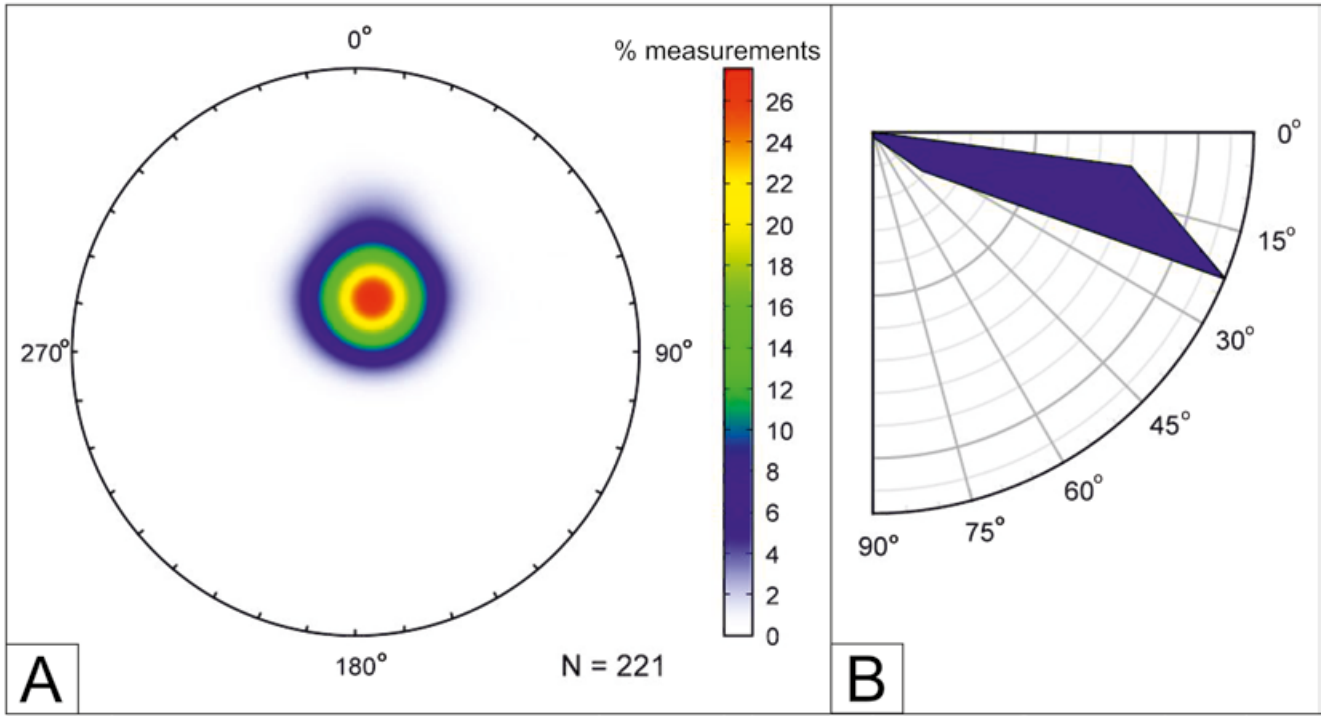

Fig. 6. Orientation of strata in the Vistula River source area. **A.** Contour plots from the stereographic projection of bedding planes (lower hemisphere, equal-area projection). **B.** Histogram of dip angles of strata.

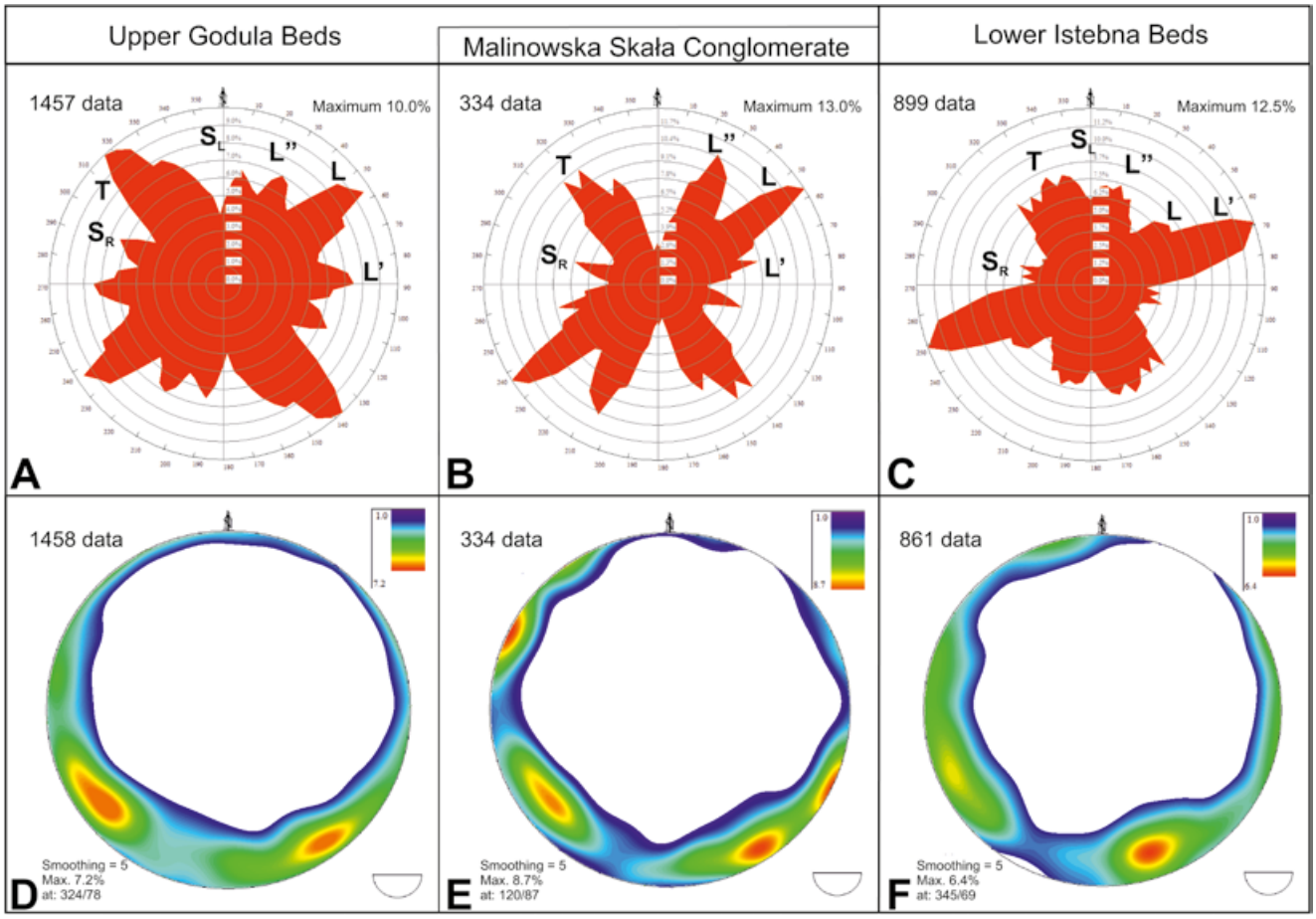

Fig. 7. Diagrams of analysed joint sets in each lithostratigraphic series in the Vistula River source area. **A**–**B.** Rose diagrams (circular frequency) of strikes of joints. **D**–**F.** Contour plots of analysed joints.

proportion of the joint population is the T set, but the diagram shows that their orientations are very scattered, ranging from 310° to 345° (Fig. 7C). The directions of the L" set (range 10° to 25°) are also widely scattered. The S_L joint strike of 345–350° is not distinguished from the scattered T joint set maxima, and the S_R joints strike to 275–285°.

Topolineaments

On the DEM, 4,563 topolineaments were distinguished. Topolineaments are more pronounced in the upper and middle parts of slopes (Fig. 8). The distribution and density of topolineaments show their uneven distribution in the area (Fig. 8B, C). The highest density of topolineaments is found on the SW-facing slopes: in the upper part of the Gościejów Valley, on the Smrekowiec Mountain, the Cienkowów Ridge, the Malinowska Skała Mountain, and in the Wątrobny Valley. Also, the topolineament density is high on the S-facing slope of the middle part of the Cienków Ridge. The lesser densities of topolineaments are found on the SW slopes of the Czupel Mountain, the Malinów Mountain and the Czarny Mountain. A comparison of the lineament density maps with the ranges of the lithostratigraphic series shows that the frequency of topolineaments depends on lithology (Fig. 8C). Topolineaments are more frequent on these slopes that are composed of the thin-bedded rocks of the UGB. However, the bedrock of some of the above-mentioned slopes also consists of the thick-bedded LIB rock series (in the central part of the Gościejów Valley, the central part of the Cienków Ridge, on the slopes of the Malinów Mountain, on the Malinowska Skała Mountain, and in the Wątrobny Valley). Therefore, it should be assumed that the appearance of topolineaments was influenced by several factors related to the bedrock. In such a case, topolineaments can be manifestations of fracture or fault zones.

The lengths of topolineaments, delineated at a scale of 1:10,000, range from 13.31 m to 912.52 m. The total length of topolineaments is 533.54 km (Tab. 2). The distribution

Table 2

Length of the topolineaments
in the Vistula River source area.

Maximal	912.52 m
Minimal	13.31 m
Mean	233.80 m
Median	89 m
Std. deviation	91.20 m
Sum	533.54 km

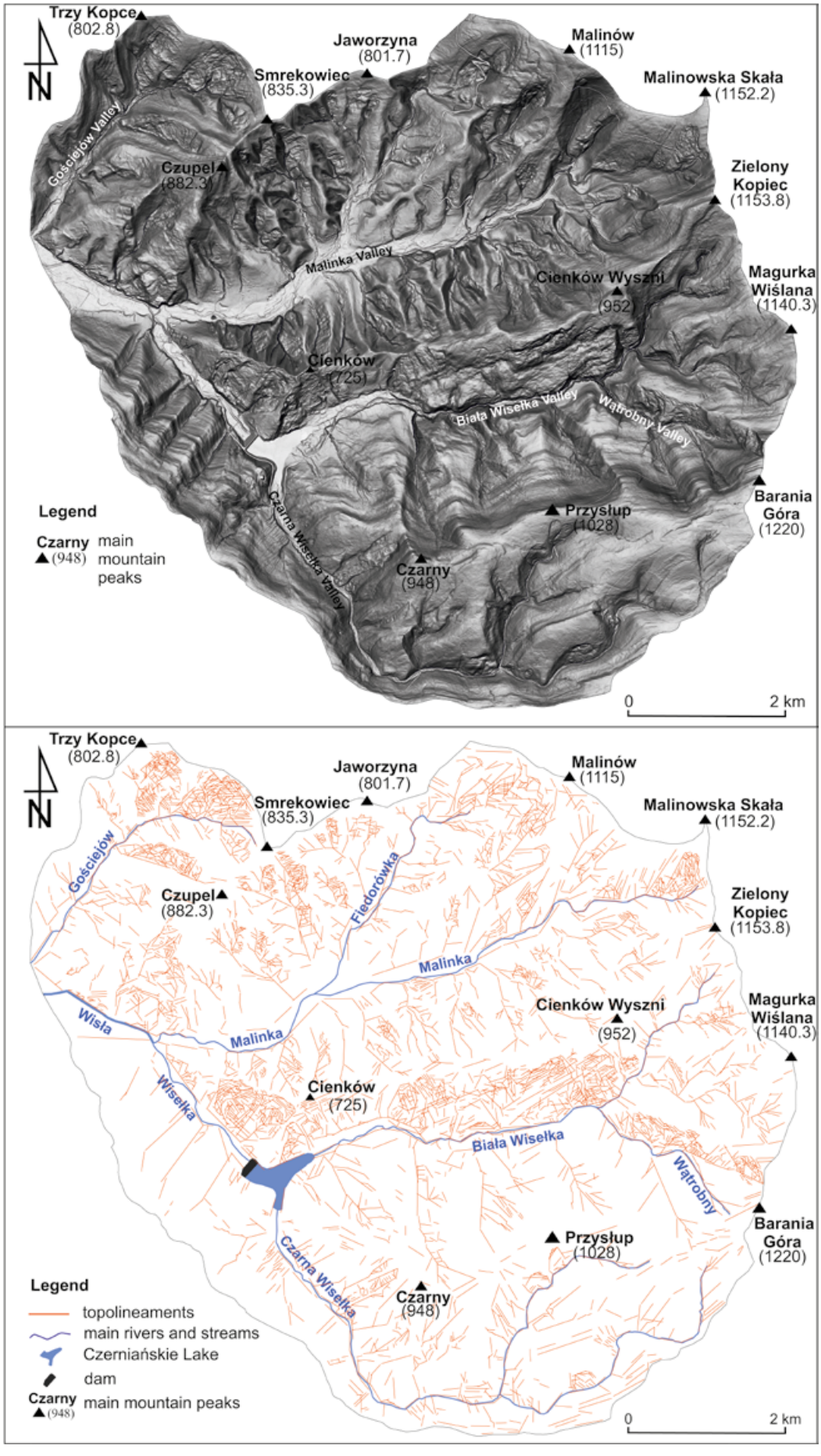

Fig. 8. Results of topolineaments extraction from LiDAR-DEM in the Vistula River source area. **A.** DEM of the study area from LiDAR data.

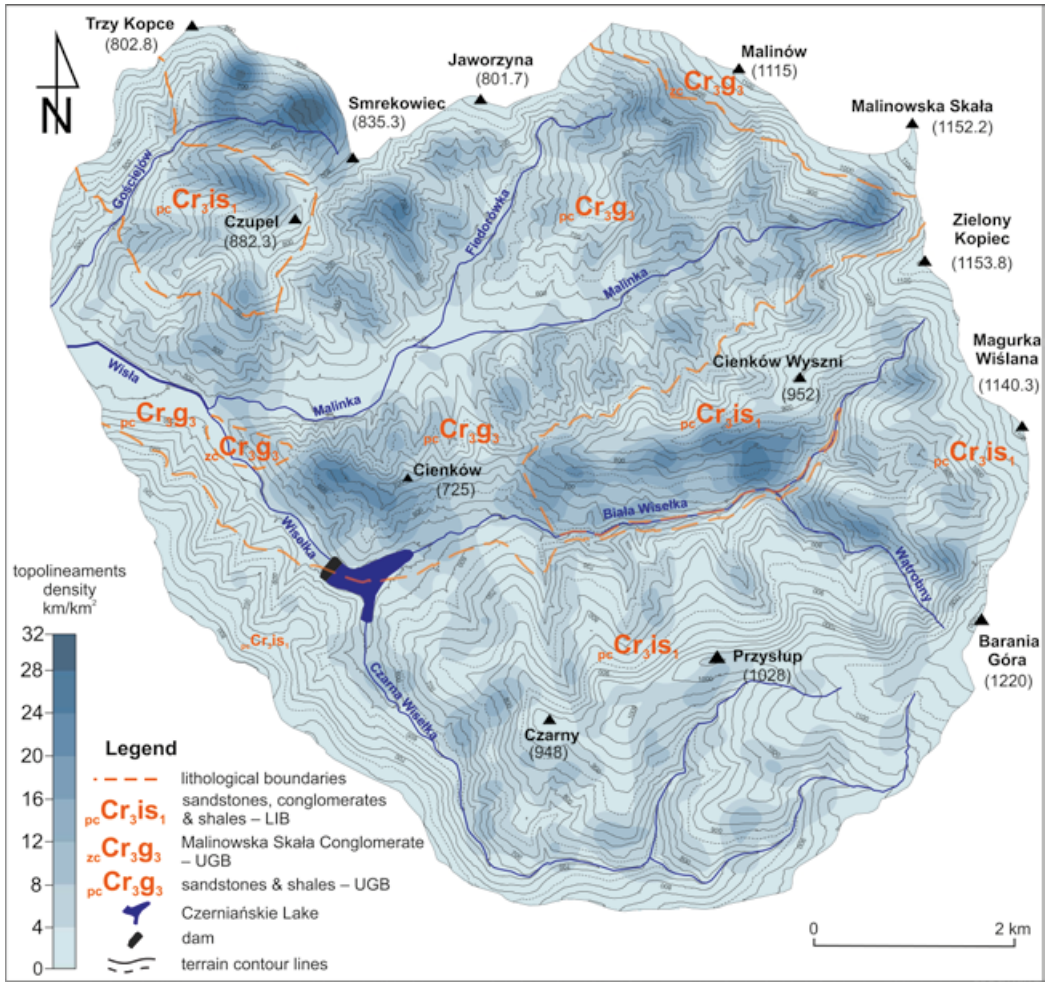

Fig. 8. **B.** Topolineaments map of the study area. **C.** Topolineaments density map of the study area against the lithological boundaries.

of topolineaments among the length classes is unimodal and right-skewed (Fig. 9). Topolineaments with lengths between 50 and 100 m are the most numerous (1,790 topolineaments). The number of topolineaments in classes above 200 m falls sharply. Only 27 topolineaments exceed 500 m in length.

In terms of orientation, the delineated topolineaments show a multimodal distribution, in which two modes are most prominent (Fig. 10). Most topolineaments strike to 310–330° (NW). This range also stands out in terms of the total length of topolineaments from 38.35 to 41.41 km, respectively. The second important orientation is broadly distributed in directions 30–80°, with the most frequent orientations in a range of 50–70° (ENE). The total length of such oriented topolineaments varies from 31.65 (30–40°) to 38.65 km (60–70°; Fig. 10).

The dominant topolineaments are mutually perpendicular (orthogonal), striking to the NW–SE (322+/-5°) and ENE–WSW (58+/-5°; Fig. 11; Tab. 3). The associated topolineaments strike to the NWW–SEE (300°), E–W (85+/-5°) and NE–SW (40+/-5°), i.e., sub-parallel to the main ones (difference in orientation up to about 20°), and are probably genetically related.

Topolineaments oriented in other directions are less pronounced in the terrain relief and are secondary to the main topolineaments. The subordinate topolineaments strike to the WNW–ESE (290°) and N–S (354°). They are oblique (diagonal) to each other, intersecting at an angle of 60° (Fig. 11). The NNE–SSW topolineaments are associated with the N–S ones; the difference in orientation reaches 20°.

The distribution of topolineament directions (Fig. 11) is similar to the joint directions (Fig. 7). The NW–SE and associated NWW–SEE topolineaments correspond to the T joint set The topolineaments, striking to the ENE–WSW and associated E–W and NE–SW-oriented topolineaments, correspond to the L and L' longitudinal joint sets. Secondary topolineaments are associated with the diagonal joint system (S_R, S_L). Topolineaments oriented WNW–ESE are related to the S_R joint set, and N–S topolineaments are related to the S_L joint set (Figs 7, 11). The NNE–SSW topolineaments can be associated with the S_L joint set or correspond to the L" set

Faults

The identification of faults in the study area was difficult for several reasons. First of all, there is a small number of outcrops, where these structures can be observed. Secondly, the low lithological variability results in the poor manifestation of faults in the cartographic image. In many cases, the

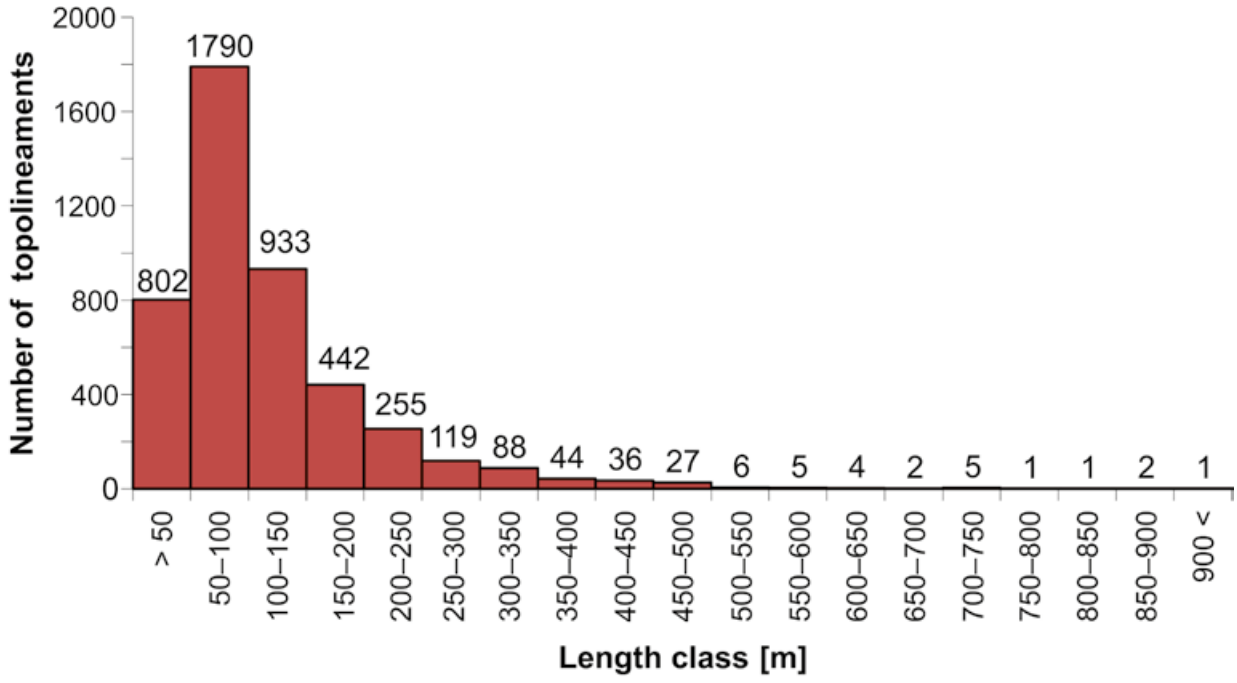

Fig. 9. Histogram of topolineament length distribution in classes.

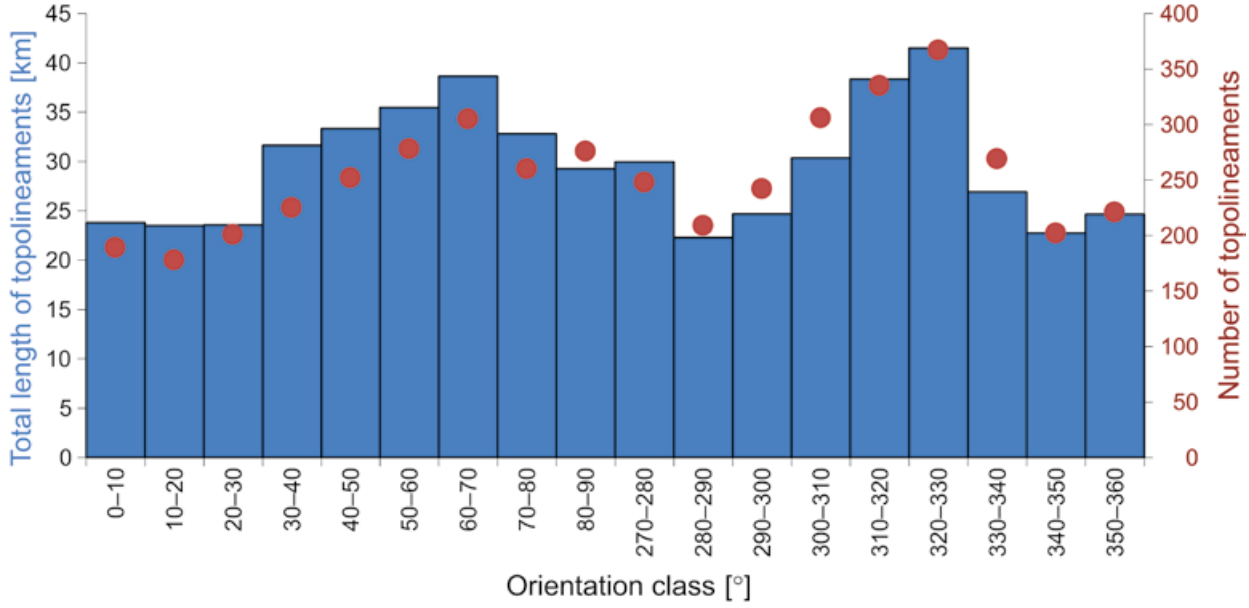

Fig. 10. Histogram of topolineament length and number with respect to orientation classes.

Table 3

Classification of topolineaments.

	Main topolineaments		**Second order topolineaments**	
Direction	NW-SE (322+/-5°)	ENE-WSW (58+/-5°)	N-S (354°)	WNW-ESE (290°)
	Associated topolineaments		Associated topolineaments	
Direction	NWW-SEE (300°)	NE-SW (40+/-5°)	NNE-SSW (15°)	–
	–	E-W (85+/-5°)	–	–
Angle system	orthogonal		diagonal	

displacement along a fault surface is too small to be shown on the scale of geological maps produced so far.

Faults are exposed on the LiDAR-DEM mainly as topolineaments, along which displacements of uncovered rock strata are visible (Fig. 12A–C). A few such N- and NW- trending faults are arranged in a sequence between the Barania Góra and the Malinowska Skała mountains in the eastern part of the area and on the slopes of the Malinów Mountain (Fig. 13). Faults also are revealed along opened fractured in the upper part of the south-western slopes of Malinów Mountain. Sometimes the presence of faults is indicated in the topography by the triangular facets (faceted spur; Cotton, 1950; Bull, 1984; Zuchiewicz and McCalpin, 2000). The best example of such a relationship occurs at the southern margin of the Malinka Valley, where some longitudinal, normal faults were identified (Fig. 12D).

Some faults are poorly marked in relief and some of them were determined on the basis of additional analysis of the strike and density of topolineaments. In such a case, topolineaments result from the gravitational rejuvenation of the fault surfaces within the bedrock (Jaroszewski and Piątkowska, 1988; Graniczny and Mizerski, 2003). On the basis of such premises, the faults and fault zones were identified along the Wisła and the Malinka valleys in the western part of the area and in the northern part between the Gościejów Valley and the Malinów Mountain (Fig. 13).

The first group of dislocations that stand out on the map are the NW–SE transverse faults (Fig. 13). Along these faults, the displacement of mountain ridges, and the extinction and disruption of other faults can be observed on DEM. Transverse faults are seldom displaced by other dislocations (usually longitudinal, ENE–WSW faults). The distribution of transverse faults in the study area is quite regular and they are arranged in fault zones.

Numerous transverse faults are exposed in the central part of the area within the Biała Wisełka Valley and the Cienków Ridge (Fig. 13). The most important zone, namely fault No. 4 marked on the DGMP (Burtan, 1972; Nescieruk and Wójcik, 2017), runs transversely to the Biała Wisełka Valley (Fig. 4), east of the Wisła Czarne settlements. In contrast to the picture on the DGMP, this zone has a discontinuous character and consists of many fault segments, several of which form a system of mutually parallel dislocations on the Cienków Ridge. These faults produce an offset of the boundary between the UGB and the LIB (Fig. 13). The relief along this fault zone is marked by numerous topolineaments, which are in fact NW–SE-trending, linear landslide scarps. In this zone, in outcrop No. 47 (on the left side of the Biała Wisełka Stream; Figs 13, 14), mesoscale, fault-related structures were found. The displacement on the fault resulted in the reorientation of rocks in the outcrop (Fig. 14B–E). Bedding planes of sandstones and mudstones of the UGB dip towards the ESE (100/30 – 114/40; Fig. 14B), i.e., they are oblique relative to strata observed in the nearby outcrops, which show a dip towards the SW. In the NNW part of the outcrop, there is a thrust surface (126/40; Fig. 14B), almost parallel to the bedding planes, which is accentuated by a several-centimetres-thick zone of schistosity with NW-vergent, asymmetrical drag folds (orientation of axial surface 130/75; Fig. 14B, E). An intense axial cleavage

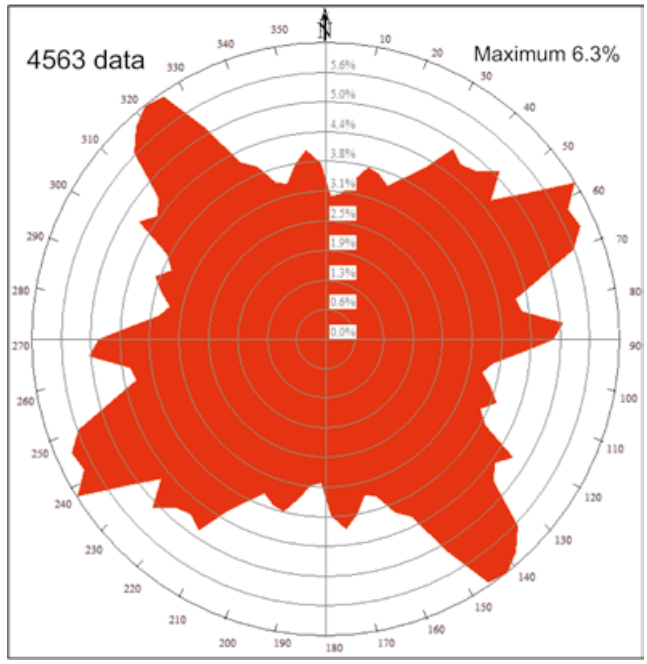

Fig. 11. Rose diagram of topolineaments in the Vistula River source area.

developed along the axial plane of these folds. The thrust surface was reactivated by a small rotational, sinistral slip of the landslide body (Fig. 14B). The landslide detachment surface runs horizontally in a SSE direction. A cylindrical slip surface with a variable orientation towards the NNW (270/20, 200/20, 234/20) eventually converges with the thrust surface. The displacement of the colluvium is small, approximately 30 cm (Fig. 14C).

It is difficult to define the relationship between the thrust-related structures and those resulting from landslide movements. Drag folds and axial cleavage indicate that the deformation is related to thrust movements, postulated by Burtanówna *et al*. (1937). On the other hand, drag folds formed in the landslide slip zone were described by Margielewski *et al*. (2007, 2008) in the Miecharska Cave. Probably both deformations contributed to the development of folds and cleavage.

Structures related to the development of thrusts in the contact zone of the UGB and LIB were documented in outcrop No. 60, in the upper part of the Biała Wisełka Valley. The presence of slickensides indicating the "top to the NW" sense of movement was recorded on the bedding planes of the LIB sandstones (Fig. 14F).

Horizontal and vertical displacements also have been documented along other transverse faults. Right-lateral displacement is indicated by the horizontal slickensides, preserved on some fault surfaces (Fig. 15A) in outcrops No. 53, 54 and 55 (the Cienków Ridge; Fig. 13). These faults have a character of single planes or brittle shear zones. Transverse faults in the outcrops described dip steeply towards the SW or NE (e.g., 50/70, 60/60, 64/60; Fig. 15). The normal-slip displacements are documented by tectonic steps and locally developed horsetail splay (Fig. 15C). Horsetail splay and fracture opening, accompanying vertical movements, indicate an extensional regime of deformation. Faults in

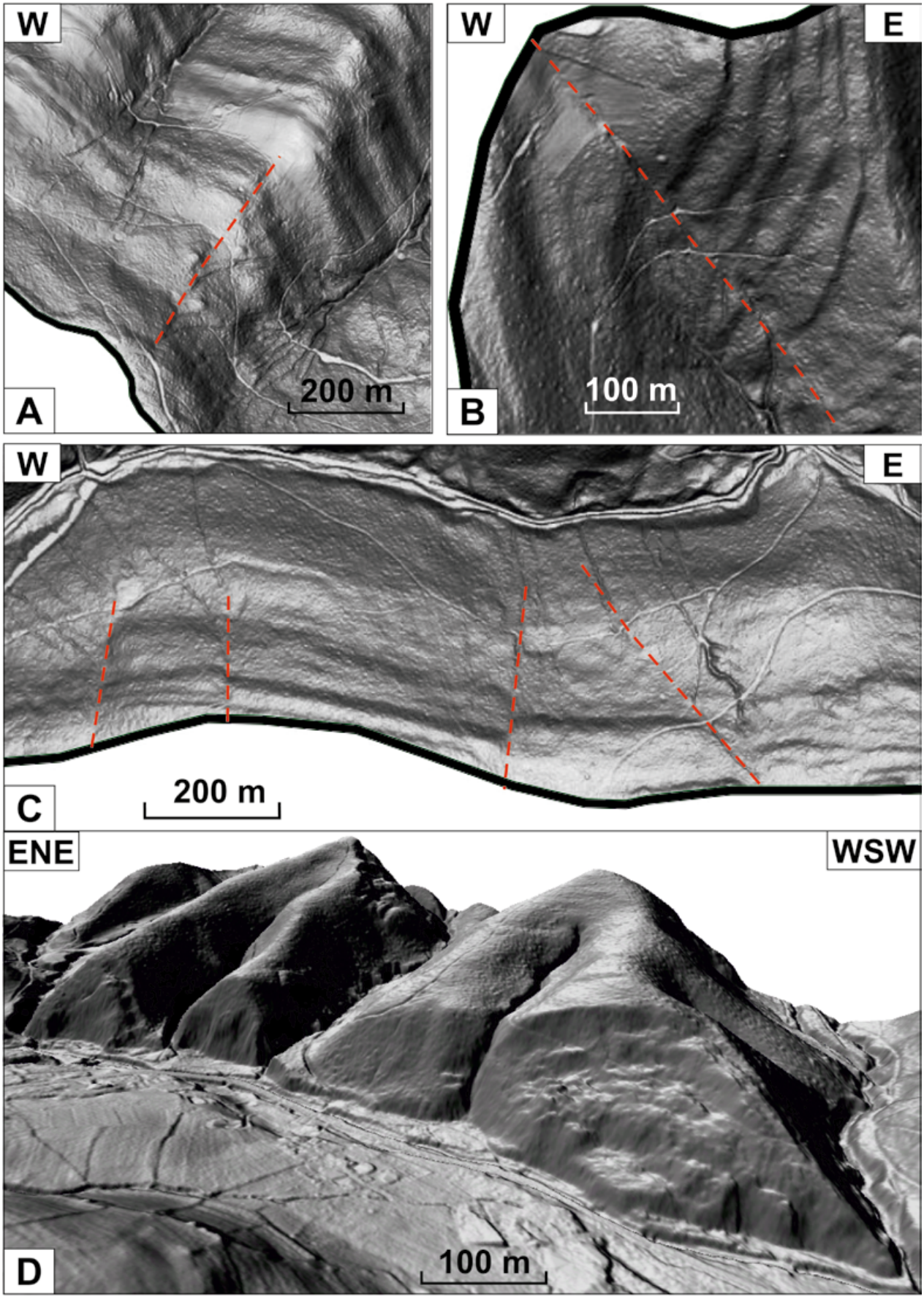

Fig. 12. Examples of faults interpreted on LiDAR-DEM of the Vistula River source area. **A.** On the south-western slopes of the Wisełka Valley. **B.** On the north-eastern slopes of the Gościejów Valley. **C.** On the southern slopes of the Czarna Wisełka Valley. **D.** Fault-related triangular configurations of slopes on the southern side of the Malinka Valley.

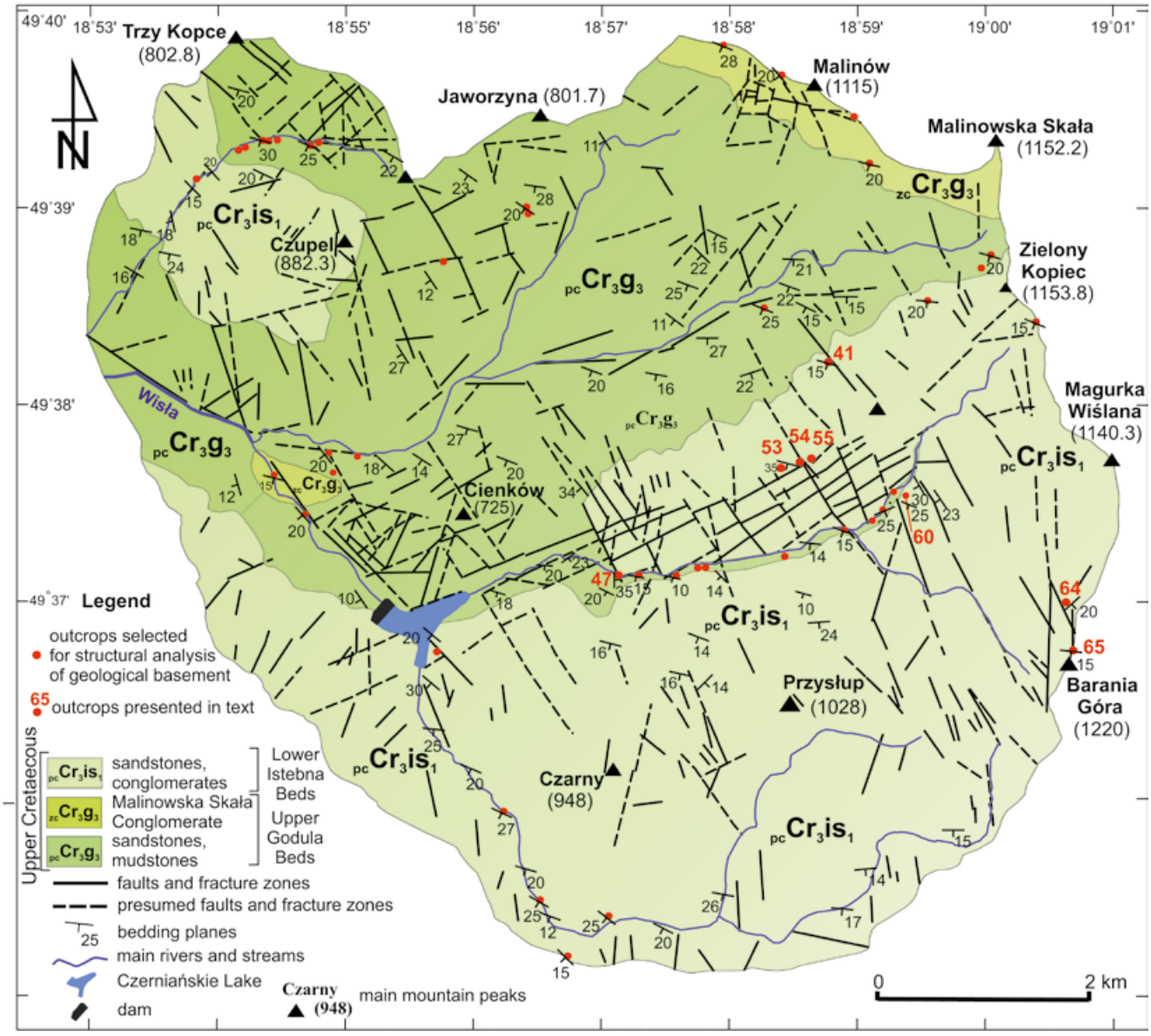

Fig. 13. Structural map of the Vistula River source area (lithostratigraphic boundaries modified after Burtan, 1972; Nešcieruk and Wójcik, 2017).

the outcrops presented form sets of conjugate pairs and the bisector of angle 2Θ between their surfaces indicates that the youngest displacements on these faults were related to vertically directed forces (Fig. 15D).

Another transverse fault zone was recognised in the middle part of the NW slope of the Cienków Wyszni Mountain, in the LIB (outcrop No. 41; Fig. 13). In the lower part of the outcrop, there are sediments of submarine gravity flows (Fig. 16A). These are dark grey, weakly consolidated claystones with sandstone clasts. They are differentiated from the overlying, thick-bedded sandstones and conglomerates. The contact between them has an orientation of 178/35 to 198/20. These rocks are cut through by numerous complementary fault planes with slickensides (Fig. 16B, C). Kinematic indicators document a strike-slip origin of the transverse faults. The dominant right-lateral sense of movement (towards the SE) is exhibited by the NWW–SEE trending faults (300°), sub-parallel to the T joint set (Fig. 16D). Dextral displacement also occurred along some N–S-striking faults (355°). On the other hand, left-lateral, oblique-slip movements (towards W) are indicated by structures present on several surfaces, oriented ENE–WSW (75°), i.e., parallel to the L joints set (Fig. 16C, D). A clear record of younger, vertical movements is the displacement of sandstone and conglomerate beds along several fault planes. As in outcrops No. 53–55, these faults form sets of conjugate pairs (Fig. 16A, B). The normal-slip displacements were mainly towards the NW and NE, the latter direction being well documented by striations on the surfaces of faults with a NW–SE direction (Fig. 16C, D). Normal-slip kinematic indicators of displacement were also observed on some fault planes, directed towards the E and SE.

The above-mentioned faults, parallel to the L and L' joint sets (longitudinal), form the second group exposed in outcrops and marked on the map (Fig. 13). The longitudinal dislocations are cut by transverse faults into a series of

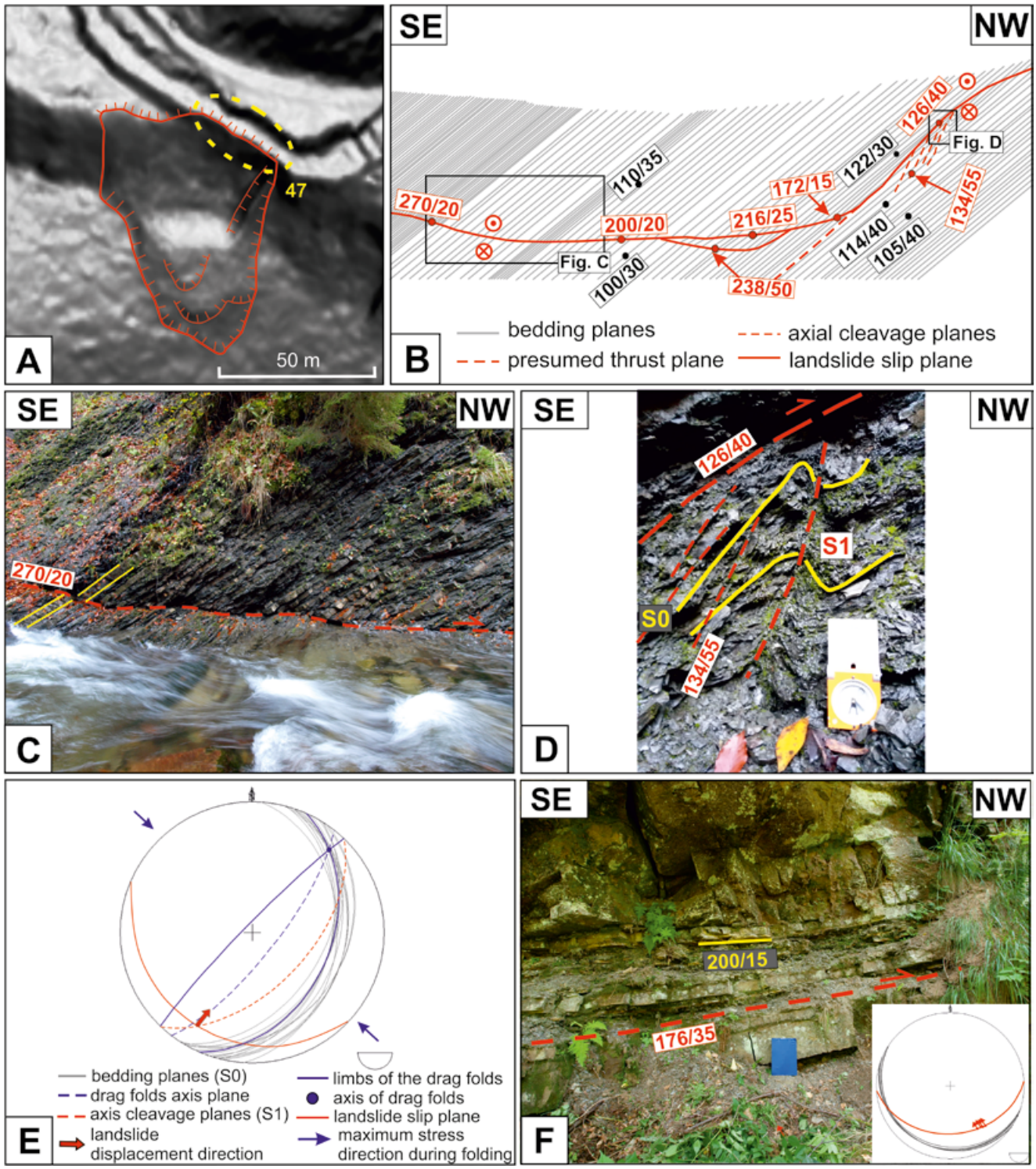

Fig. 14. Structural features exposed in the Biała Wisełka Valley. **A.** Landslide along the NW–SE-trending fault zone in the Upper Godula Beds (fault No. 4 on Fig. 3) and location of outcrop No. 47. **B.** Structural sketch of outcrop No. 47 with the kinematic interpretation of the sliding surface. **C.** Photograph of outcrop No. 47. **D.** Drag folds and axial cleavage planes at the bottom of the thrust plane in the NW part of outcrop No. 47. **E.** Stereoplot of the bedding planes and tectonic structures in outcrop No. 47 with the kinematic analysis of displacements. **F.** The Lower Istebna Beds outcrop (No. 60) with the stereoplot of the bedding planes and a thrust plane with a "top-to-NW" sense of movement, oblique to the bedding, in outcrop No. 41.

offset segments. These faults are most clearly exposed on the south-eastern slope of the Cienków Ridge. The slope has a large number of topolineaments (Fig. 8), which may indicate the presence of a wide ENE–WSW-oriented fault zone. They are several hundred metres long and form high (up to 50 m) morphological thresholds, along which landslide escarpments developed (vide Sikora, 2018).

Among the faults, which can be associated with the longitudinal joint sets, dislocations of NNE–SSW strike, i.e., along the course of the L" joints are the least frequent.

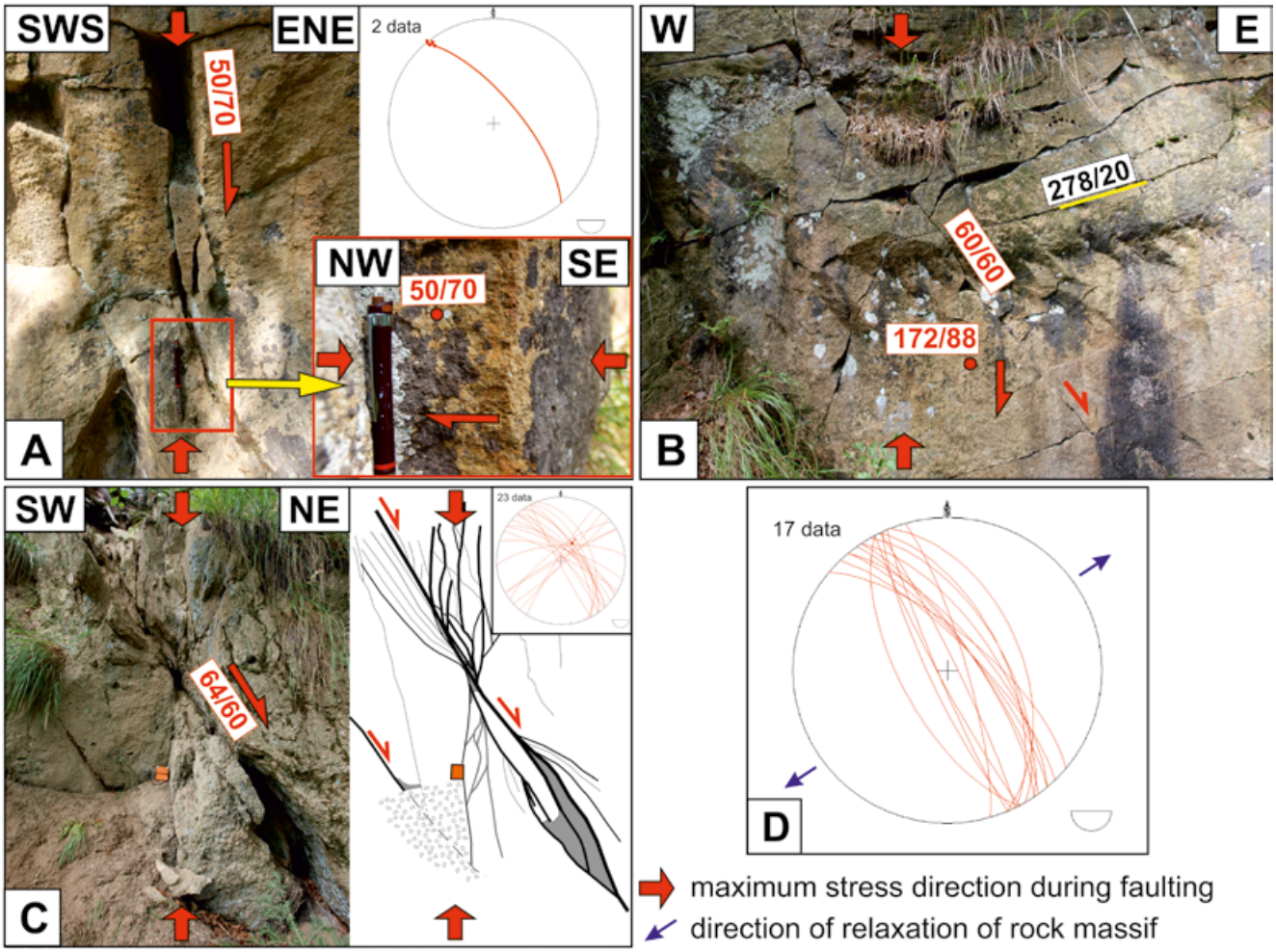

Fig. 15. Transverse faults exposed in the LIB outcrops on the crest of the Cienków Ridge. **A.** Dextral NW–SE-trending oblique-slip fault, overprinted by a normal dip-slip fault (outcrop No. 55). **B.** Normal NE-dipping fault visible on the longitudinal ENE–WSW trending fault surface (outcrop No. 55) **C.** Transverse fault zone with well-developed horsetail splay structure as a result of younger normal dip-slip faulting (outcrop No. 54). **D.** Stereoplot of the transverse fault planes exposed in outcrops No. 53–55. Half arrows show the sense of displacement of the hanging wall or absent wall of the faults.

They are most distinct in the upper part of the Gościejów Valley and several dislocations of this type were recorded on the SW slopes of the Malinów Mountain, in the eastern part of the study area (Fig. 13).

A zone of high joint density in the LIB sandstones is oriented NNE–SSW on Barania Góra Mountain (outcrop No. 65; Fig. 17). The density of fractures and the small tectonic structures present on their surfaces indicate the existence of an oblique-slip, brittle shear zone. The outcrops are dominated by N–S trending joints of the S_L set In places, there are slickensides with striations, indicating left-lateral displacement. Slickensides and kinematic indicators are more common on the surfaces of the NE–SW-oriented joints of the L" set, which are consistent with sinistral displacements toward the SW (Fig. 17B–D). The poor exposure of the zone in the field and its equally poor exposure in the slope relief lead to the conclusion that it is similar to hidden fault zones. Such a hidden fracture zone is prone to landslide occurrence and other mechanical disruptions of a rock massif. North of the outcrop, landslide processes actually took place.

Along this zone in outcrop No. 64, which is located 400 m from outcrop No. 65, there is a steep (Fig. 13), locally vertical rock escarpment (up to 27 m high) of the landslide known as the "Czerwony Usyp" (Fig. 18). The orientation of the wall corresponds to the fault plane, which is parallel to the N–S-trending S_L joint set In its vicinity, a transverse NW–SE fault (Fig. 13) is marked. At the bottom of the outcrop, there is an intercalation of thin-bedded LIB flysch rocks, above which there is a 15-m-thick package of the Istebna conglomerates (Fig. 18A). As in the other examples mentioned above, this outcrop also shows a record of successive, tectonic events. Within the thin-bedded sandstones, a mesoscopic, syndepositional (isoclinal and tight) fold, overturned to the NE (fold axis orientation 124/32; Fig. 18B), occurs. Structural studies have concluded that these rocks have undergone subsequent shear deformation. Diagonally to the axial surface of the fold and approximately parallel to the orientation of the strata in its upper limb, a "top to the NW" thrust plane was observed (Fig. 18B, C). It is emphasised by a slight offset of the layers in both limbs of the thrust.

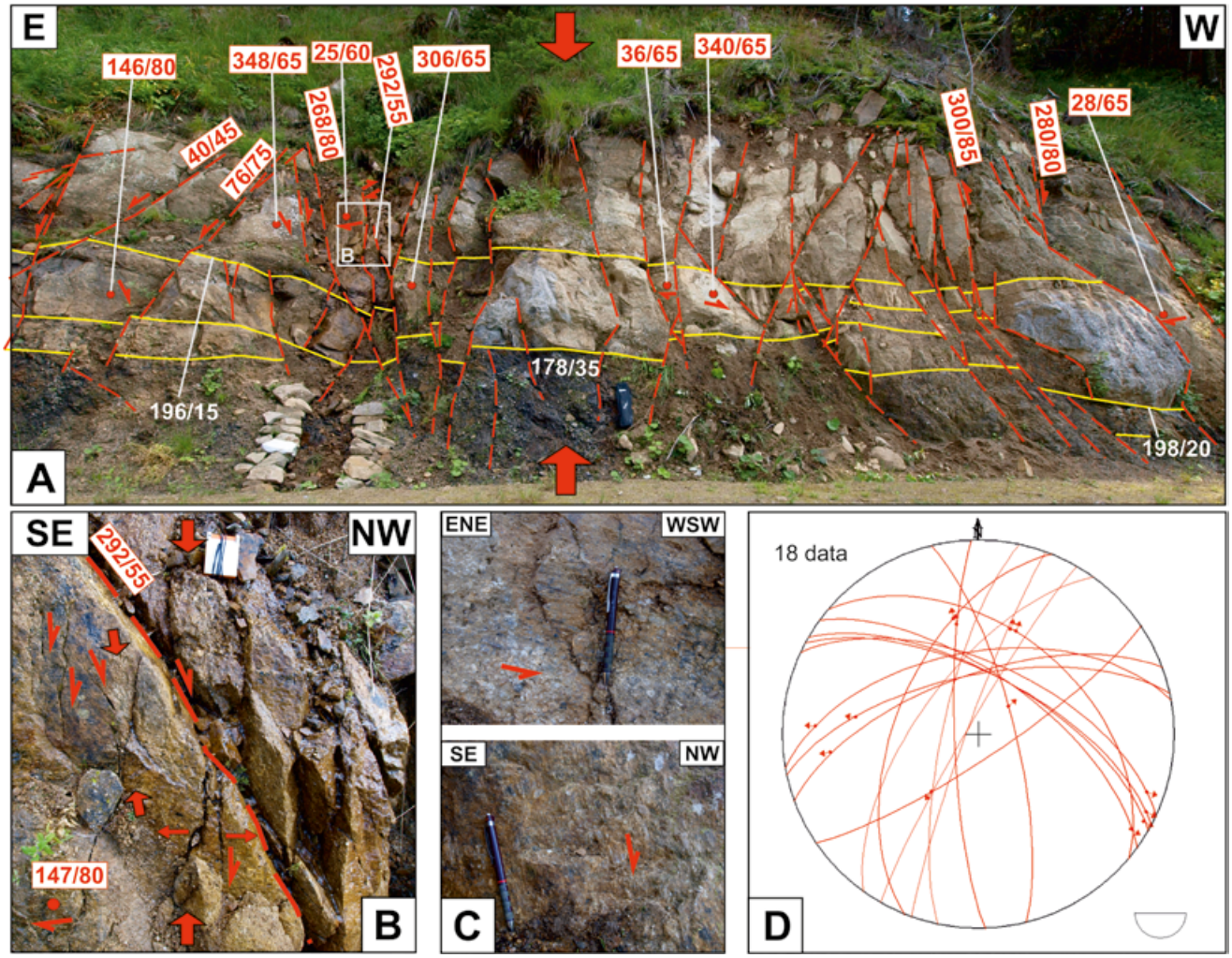

Fig. 16. Fault zone exposed on the NW slopes of the Cienków Ridge in the LIB rocks (outcrop No. 41). **A.** Photo with marked transversal fault planes and bedding planes. **B.** Example of superposition of the transverse and longitudinal faults. Brittle shear zone with open Riedel shear fractures, related to the NW-dipping normal-slip displacements along the longitudinal ENE–WSW trending fault, is visible on the dextral NW–SE trending fault surface. **C.** Examples of surfaces with the striae related to strike-slip faulting along the longitudinal fault and normal-slip faulting along the transverse fault. **D.** Stereo plot of the fault planes in outcrop No. 41. For explanation of arrows, see Figures 12 and 13.

Faults in statistical terms

In total, 403 faults with a total length of 159.10 km were identified in the study area (Tab. 4). The length of the longest faults is 1.99 km and the shortest is 65.76 m long. Faults in the study area mostly reach lengths between 150–400 m (Fig. 19). These represent 56.33% of all faults. The proportion of faults longer than 500 m decreases with the increase of their length and only 10 exceed 1 km.

The results of field studies showed that the orientation of faults corresponds to the directions of joint sets, but the rose diagram of fault orientations shows that their directions are more regular (Fig. 20). The small dispersion of fault directions indicates that faults parallel to the orientation of joints of the orthogonal system are the most distinct in the study area. Moreover, the diagram confirms the prevalence of transverse faults over the other dislocations.

The multi-modal distribution of the number and total lengths of faults in the orientation classes (Fig. 21) confirms that, quantitatively, the best-represented group are the faults that correspond to the orthogonal joint system of the T, L and L' sets. These are the NW–SE (in the range 320–330°), the NNW–SSE (in the range 330–340°) transverse faults, and the ENE–WSW longitudinal faults (in the range 50–70°). Within a narrower range, the NW–SE faults (320–330°) also are prominent in terms of the total length (24 km).

Table 4

Length of faults.

Maximal	1993 m
Minimal	65.76 m
Mean	394.79 m
Median	327 m
Std. deviation	252.60 m
Sum	159.10 km

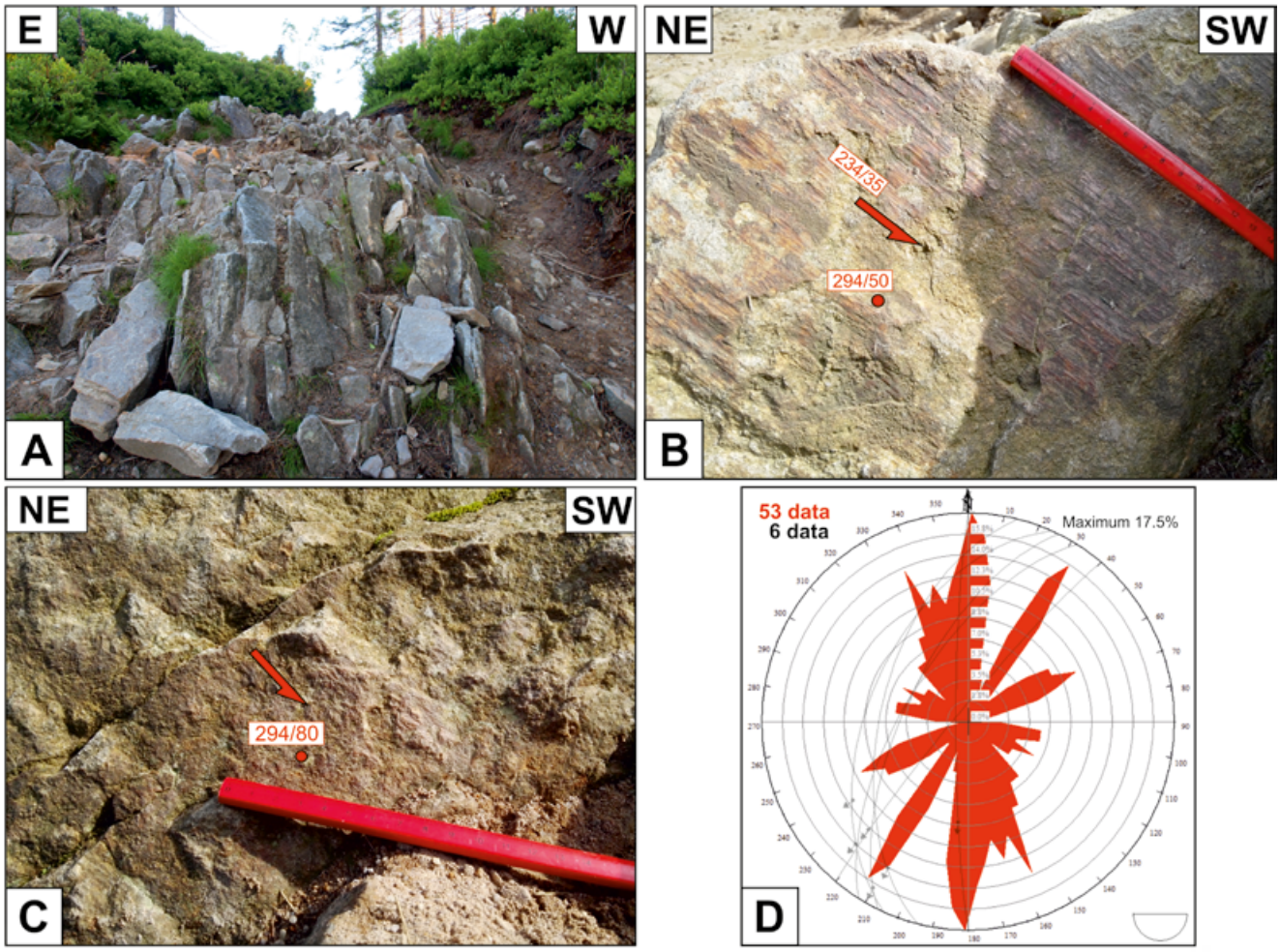

Fig. 17. Fracture zone related to the sinistral strike-slip and oblique-slip brittle-shear zone in the LIB rocks exposed on the northern slope of the Barania Góra Mountain (outcrop No. 65). **A.** Intensely jointed sandstones. **B.** Slickenside with striae documenting the sinistral oblique-slip sense of movement of the fault. **C.** Fault plane with tectonic steps related to the R fractures. **D.** Combined diagram with the circular distribution of joints and stereoplot of the fault planes in outcrop No. 65. For explanation of arrows see the Figures above.

The length of the ENE–WSW longitudinal faults (60–70°) is 15 km (Fig. 21).

Faults with intermediate directions or corresponding to the directions of other joint sets are fewer both in terms of a number and total length on the map. In this group, faults with directions close to N–S (350–0°) stand out, corresponding to the orientation of the S_L joint set of the diagonal system. The NNE–SSW faults (10–20°), the orientation of which is similar to that of the L" joints set, are also marked. There are only a few faults with orientations consistent with the S_R joints set It is noteworthy that a very small number of faults with the WNW–ESE direction were recorded, in the range of 280–300° (Fig. 21).

Comparing the above data with the classification of topolineaments, contained in Table 3, it should be concluded that the most prominent, transverse (NW–SE) and longitudinal (ENE–WSW) faults correspond primarily to the main topolineaments, occurring in the orthogonal system, and to a lesser extent to the associated topolineaments (NE–SW and NNE–SSW). Very few faults, usually N–S, coincide with secondary topolineaments.

DISCUSSION

The data presented above confirm a monoclinal geometry of strata that dip to the SW, but the bedrock structure in the study area is more complicated than previously thought. The UGB outcrops are much more fractured than the LIB rocks. This is due to the differences in lithological composition and the contrasting thicknesses of the layers. The pattern of joint sets is consistent with the results of Mastella and Konon (2001, 2002) and Tomaszczyk (2005). Despite the demonstrated differences in the degree of jointing, the same regular network of joints exists in both rock series, along which faults, fault zones and hidden fractures zones developed. The differences in the orientation of joint sets between the lithostatigraphic units indicate that the LIB were clockwise-rotated, relative to the UGB during thrusting of the Silesian Nappe. On the other hand, flexural-slip-related striation and shear indicators, observed in the sandstones of the LIB, show generally a "top-to-the NW" sense of movement. Accordingly, clockwise rotation of the LIB was preceded by NW-directed thrusting. Moreover, during the rotation,

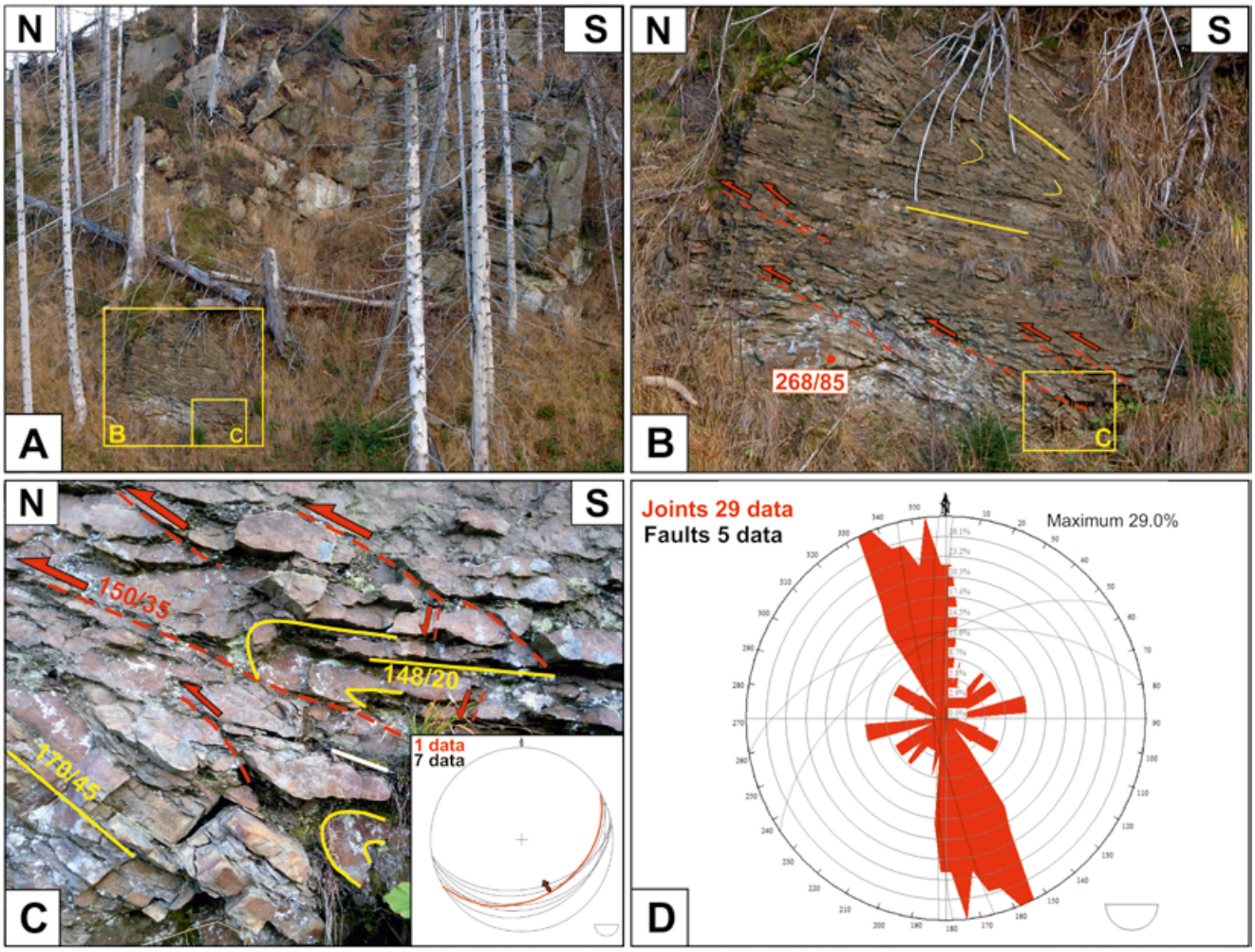

Fig. 18. The rocky scarp of the Czerwony Usyp landslide (outcrop No. 64 in the LIB rocks). **A.** Location of the thin-bedded sandstones, which are covered by the thick-bedded sandstones and conglomerates. **B.** Overturned syn-sedimentary folds with the NW-trending thrust-related shear planes. **C.** Superposition of the faulted strata and thrust shear planes. For explanation of arrows, see the Figures above. **D.** Combined diagram with the circular distribution of joints and stereoplot of the fault planes in outcrop No. 64.

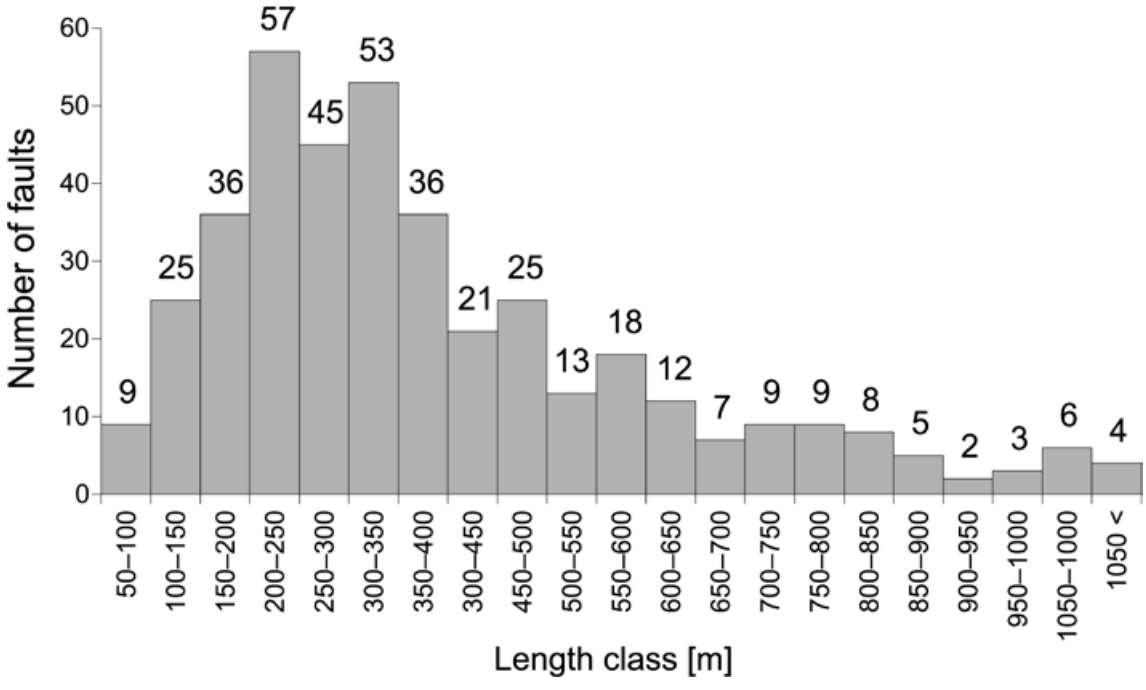

Fig. 19. Histogram of distribution of fault length.

the T joint set was dispersed (220–240°) in the thick-bedded horizons within the LIB and the L' set was better developed then the L joint set

The numerous NW–SE transverse faults identified and the newly recognised NE–SW and ENE–WSW longitudinal faults show directions consistent with the trends of the dominant joint sets of the orthogonal system: the transverse T joints set (relative to the axis of regional fold structures) and the longitudinal sets L and L'. The transverse faults (NW–SE) studied often show right-lateral kinematics. This feature was noticed earlier by Aleksandrowski (1989), Decker *et al*. (1997), Mastella and Szynkaruk (1998), Tokarski *et al*. (1999), Neścieruk (2001) and Mastella and Konon (2001, 2002), who ascribed it to the clockwise rotation of the Carpathian nappes in the Neogene. Left-lateral displacement along some of the longitudinal faults also was found; according to Tokarski *et al*. (1999), this took place in the final stage of rotation of the nappes. Indicators of a horizontal sense of movement on the fault surfaces are overprinted by structures, indicative of later, vertical movements. This proves that the later structural evolution of the bedrock was related to regional collapse of the orographically elevated rock massif (e.g., Zuchiewicz, 2001; Jankowski and Margielewski, 2022). In this phase of development of the bedrock structure, surfaces of all joint sets (orthogonal and diagonal systems) were reactivated as extensional structures and along their surfaces normal faults were developed (Tokarski *et al*., 1999; Mastella and Konon, 2001, 2002). The results obtained allow the presentation of a new model of the fault and joint system in relation to the axis of the Szczyrk Anticline (Fig. 22).

The discontinuous structures were recognised precisely in the course of topolineament analysis, based on the LiDAR data. It allowed for a new, comprehensive view of the bedrock structures in the topography and identification

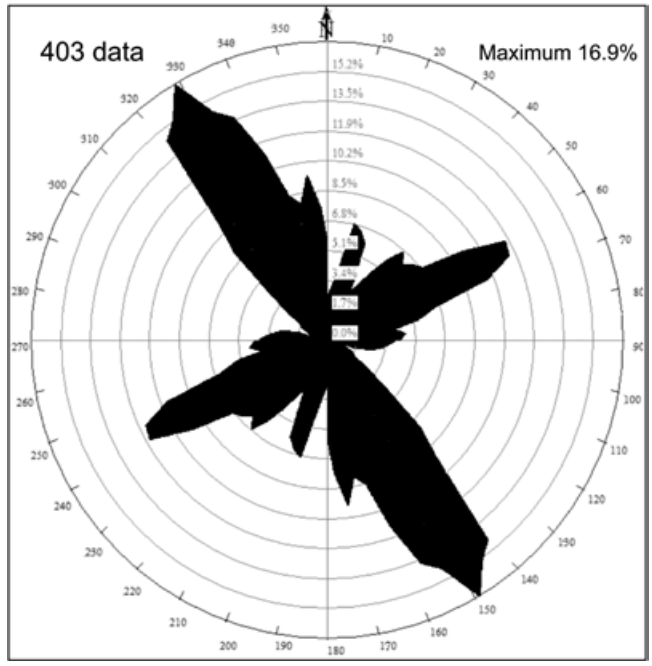

Fig. 20.` Rose diagram of faults in the study area.

of numerous new faults and fault zones. The latter are manifested as numerous topolineaments, visible in the relief of slopes in the study area. They have the same strike as faults and fractures. The most common are topolineaments, oriented parallel to the joints of the orthogonal system: T (NW–SE) and L, L' and L" (NE–SW, ENE–WSW and NNE–SSW). On the other hand, analysis of topolineament strikes and maxima of their densities, together with the detailed studies in the outcrops, allowed identification of zones that are poorly exposed in the topography. The density of topolineaments indicates zones of brittle deformation (brittle

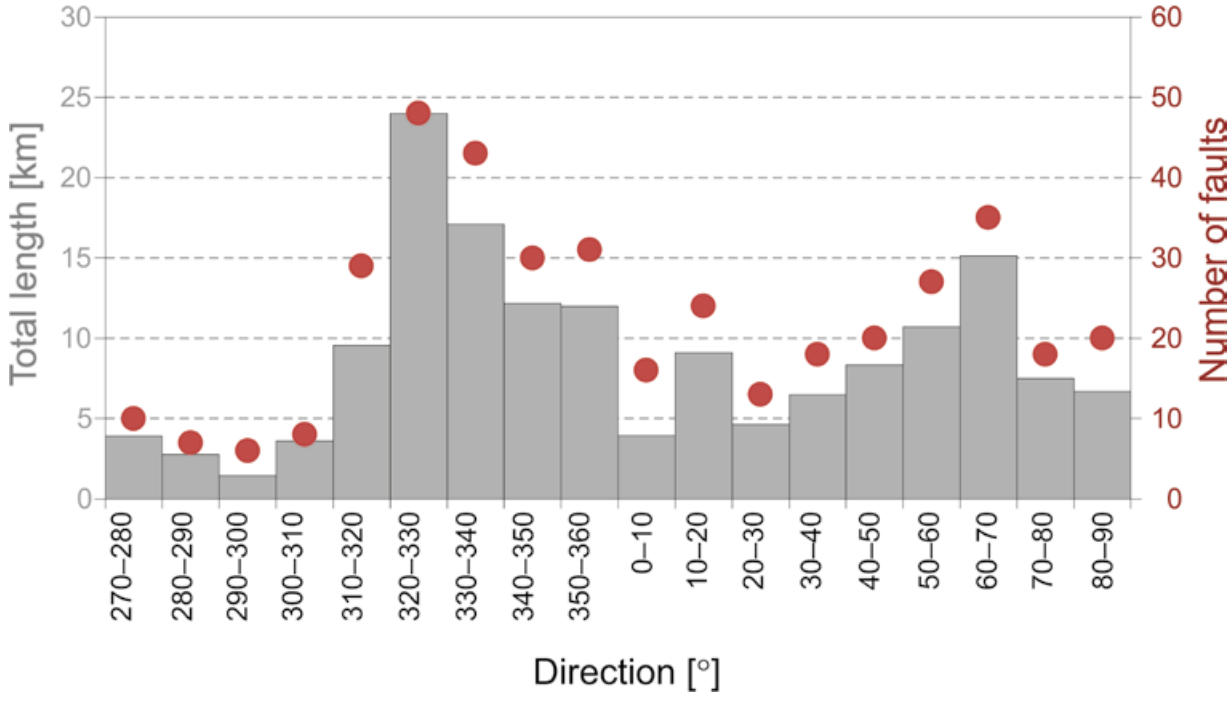

Fig. 21. Histogram of fault length and the number of faults by directions

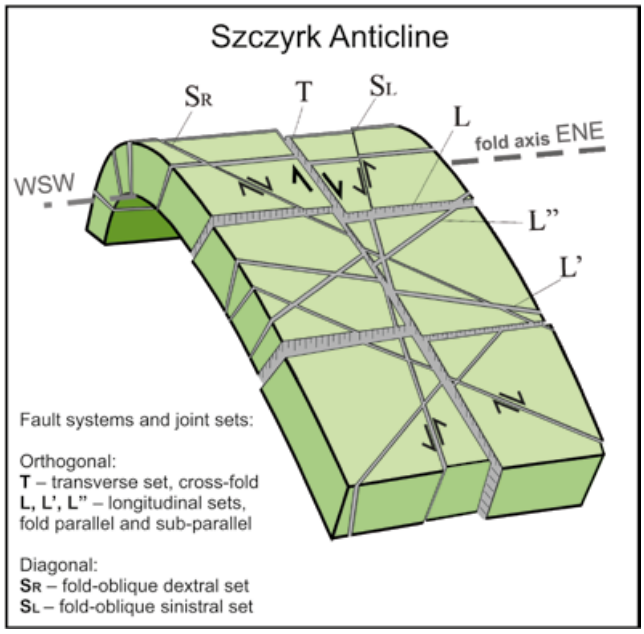

Fig. 22. Model of joint sets and fault systems within the Szczyrk Anticline.

shear zones). They may reflect mechanical weakening of the bedrock, leading to intensification of processes connected with, among others, landslide development (Sikora, 2017). The existence of similar zones (hidden fault zones) was confirmed in seismically active areas in various parts of the world (Bottari *et al*., 2020; Tusikova *et al*., 2020; Nemati *et al*., 2021). In Poland, previous studies of lineaments were based of topographic maps, air photos, radar or altimetric terrain models (Doktór *et al*., 1988; Jaroszewski and Piątkowska, 1988; Graniczny, 1989, 1994; Badura, 1996; Graniczny and Mizerski, 2003; Ozimkowski, 2008). This study has shown that the analysis of topolineaments, based on the LiDAR-DEM, gives satisfactory results, when determining faults and fracture zones. However, it should be preceded by good recognition of basic, tectonic structures, such as joints and their systems in the bedrock.

Thrust in the Biała Wisełka Valley and Gosciejów Syncline – revision

The structural studies did not unequivocally confirm the existence of an N-vergent thrust and an anticline in the top part of the UGB in their outcrops in the Biała Wisełka Valley, postulated by Burtanowna *et al*. (1937). Frequently observed calcite and quartz slickensides on the bedding planes indicate a flexural-slip towards the N–NW. Locally, minor asymmetric drag folds are also evident, but no distinct surface was found that could be considered to be a significant thrust. Similarly, no evidence of a N-vergent fold within the UGB was found in this area (vide Burtanówna *et al*., 1937).

The monoclinal geometry of bedding planes contradicts the view of Burtan (1972) and Nescieruk and Wójcik (2016) on the presence of the Gościejów Syncline in the NW part of the study area. The presence of a fold was not confirmed by the LiDAR-DEM analysis. The image shows parallel LIB outcrops with different thicknesses of strata, without folding of these layers (Fig. 23).

The Lower Istebna Beds in the NW part of the study area form an isolated patch. The analysis of their range, the orientation of layers and the relief of slopes on topographic maps and the LiDAR-DEM showed that the LIB outcrops in the Gościejów Valley are situated at a higher topographic level than these rocks, located in the southern

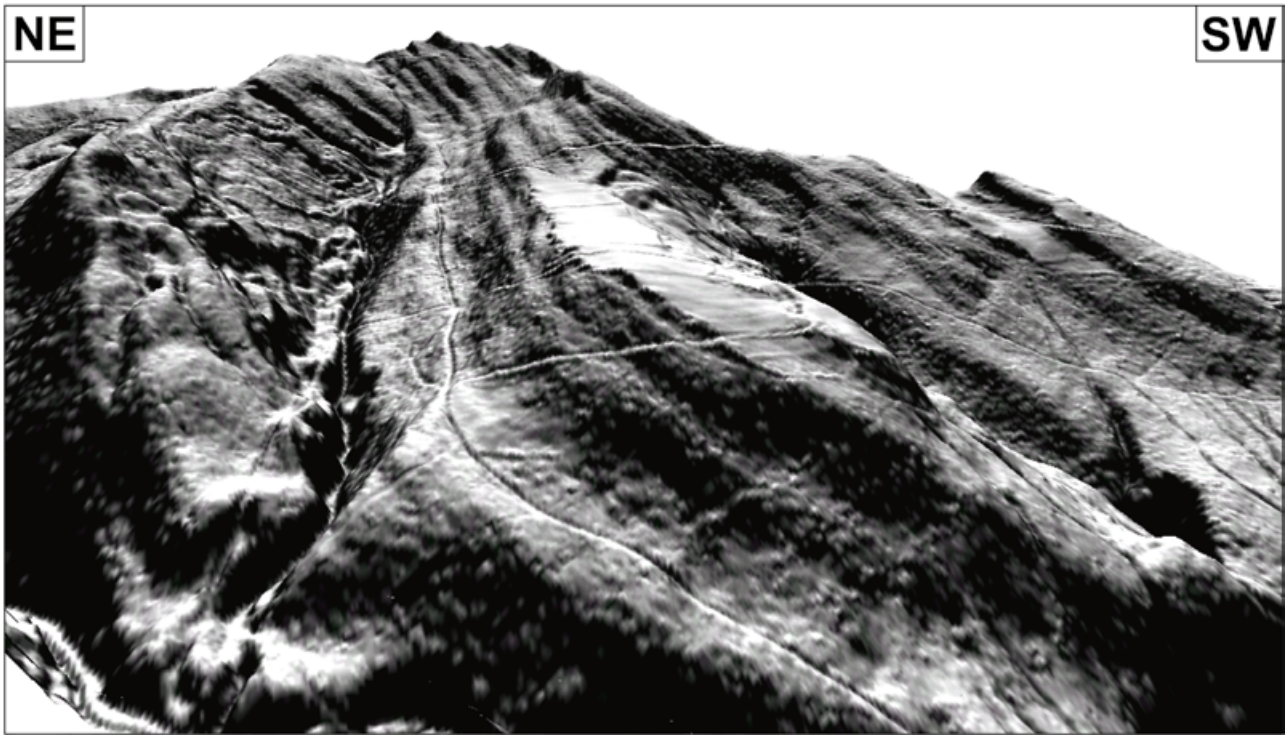

Fig. 23. Clearly visible monoclinal structure of bedrock in the Gościejów Valley on the LiDAR-DEM.

part of the area. Both these outcrops are separated by deep, sub-sequential cuts of mountain streams and depressions, developed in the rocks of the UGB, that are less resistant to erosion. Geologically, isolated outcrops of the LIB are separated also by a series of ENE–WSW-trending faults, which were also indicated by Neścieruk and Wójcik (2016, 2017). These data allow consideration of the LIB outcrop in the Gościejów Valley as a remnant of a continuous horizon, which originally covered the whole area of the lower UGB. It is difficult to state unambiguously whether it has the character of a klippe, in accordance with the concept of Burtanówna *et al*. (1937) and Burtan (1972). Therefore, this issue requires further detailed field studies.

CONCLUSIONS

Detailed structural studies, supported by analysis of the digital elevation model from LiDAR data, including the analysis of topolineaments, were the key to recognition of the structural pattern in the source area of the Vistula River (Barania Góra Mountain area). A new interpretation of the southern limb of the Szczyrk Anticline is proposed, with a systematic joint pattern. Among the 6 identified joint sets, the joints of the orthogonal system (T, L, L' and L') are the most common. The thin-bedded UGB are most affected by each of the joint sets, especially the T joint set The T joints within the LIB were dispersed by 20° during the clockwise rotation of the Silesian Nappe. The numerous, documented faults and fault zones relate mainly to the orthogonal arrangement of transverse and longitudinal joint sets relative to the axis of the Szczyrk Anticline.

The monoclinal rock outcrops are displaced mostly by transverse faults, which showed right-lateral strike-slip kinematics. Longitudinal faults may have originally exhibited left-lateral strike-slip kinematics. Faults parallel to the joints of the diagonal system (S_L and S_R) also were identified in the study area. Usually, these faults are hardly distinguishable in the relief. Among the faults, related to joints in the diagonal system, dislocations associated with the S_L joint set constitute the larger population. Their kinematics was sinistral.

Indicators of horizontal fault displacements were overprinted by those documenting vertical displacements. The change in displacement kinematics was related to the transition from a transpressional thrust tectonic regime to movements associated with an extensional regime, caused by the gravitational collapse of the nappe pile. Multidirectional reactivation of dislocations in the Polish Outer Carpathians, caused by gravitational collapse, was indicated by Tokarski *et al*. (1999).

The results of the present study indicate that zones with a high density of joints, atypical for thick-bedded rocks, are characteristic of hidden fracture zones. The latter may have an impact on the disintegration of the rock massif and the development of landslides, producing geological hazards (Weidman *et al*., 2019). In this respect, structural studies have a practical dimension, as the recognition of such zones may be of great importance for engineering works and the design of construction projects.

A problem that requires further study is the relationship between the structure of the bedrock and mountain relief and the development of landslides, significant numbers of which have been documented in the area (Sikora and Piotrowski, 2013a, b; Sikora, 2022). Selected examples from the study area (Sikora, 2018) indicate relationships between tectonics and mass movement.

Acknowledgments

This study received financial support from the Polish Geological Institute – National Research Institute project 61-2306-1201-00-0. I would like to thank A. Wójcik for his support during the realisation of the research project. I am also grateful to G. Heja and an anonymous reviewer for their critical reading and remarks, which helped to improve the paper. Frank Simpson is thanked for linguistic editing of the manuscript.

REFERENCES

Aleksandrowski, P., 1985. Structure of the Mt. Babia Góra region, Magura Nappe, Western Outer Carpathians: An interference of West and East Carpathian fold trends. *Annales Societatis Geologorum Poloniae*, 55: 375–422.

Aleksandrowski, P., 1989. Structural geology of the Magura Nappe in the MT. Babia Góra region, Western Outer Carpathians. *Studia Geologica Polonica*, 96: 7–149. [In Polish, with English summary.]

Aleksandrowski, P., 1992. Drobne uskoki i strefy ścinania. In: Mierzejewski, M. P. (ed.), *Badania elementów tektoniki na potrzeby kartografii wiertniczej i powierzchniowej*. *Instrukcje i metody badań geologicznych Państwowego Instytutu Geologicznego*, 51: 105–115. [In Polish.]

Andreucci, B., Castelluccio, A., Jankowski, L., Mazzoli, S., Szaniawski, R. & Zattin, M., 2013. Burial and exhumation history of the Polish Outer Carpathians: Discriminating the role of thrusting and post-thrusting extension. *Tectonophysics,* 608: 866–883.

Badura, J., 1996. Morphotectonics of the Żytawa-Zgorzelec Depression (SW Poland). *Przegląd Geologiczny*, 46: 1239–1243. [In Polish, with English summary.]

Badura, J. & Przybylski, B., 2005. Application of digital elevations models to geological and geomorphological studies – some examples. *Przegląd Geologiczny*, 53: 977–983. [In Polish, with English summary.]

Balla, Z., 1987. Tertiary paleomagnetic data for the Carpatho-Pannonian region in the light of Miocene rotation kinematics. *Tectonophysics*, 139: 67–98.

Barmuta, J., Starzec, K. & Schnabel, W., 2021. Seismic-scale evidence of thrust-perpendicular normal faulting in the Western Outer Carpathians, Poland. *Minerals,* 11: 1252.

Bażyński, J. & Graniczny, M., 1978. Fotolineamenty i ich znaczenie w geologii. *Przegląd Geologiczny*, 26: 288–296. [In Polish.]

Bober, L., 1984. Landslide areas in Polish Flysch Carpathians and their connection with the geological structure of the region. *Biuletyn Instytutu Geologicznego*, 340: 115–161. [In Polish, with English summary.]

Boretti-Onyszkiewicz, W., 1968. Joints in the Flysch of Western Podhale. *Acta Geologica Polonica*, 18: 101–152. [In Polish, with English summary.]

Bottari, C., Giammanco, S., Cavallaro, D., Sortino, F., Scudero, S., Amari, S., Bonfanti, P., Daolio, M. & Groppelli, G., 2020. How to reveal unknown hidden faults and historical earthquake damage applying multidisciplinary methods in archaeological sites: The case of mid- third century CE Mt. Etna earthquake (Eastern Sicily, Italy). *Tectonophysics*, 790: 228555.

Bull, W. B., 1984. Tectonic geomorphology. *Journal of Geological Education*, 32: 310–324.

Burtan, J., 1972. *Szczegółowa Mapa Geologiczna Polski, arkusz Wisła 1:50 000*. Wydawnictwa Geologiczne, Warszawa. [In Polish.]

Burtan, J., 1973. *Objaśnienia do Szczegółowej Mapy Geologicznej Polski, arkusz Wisła 1: 50 000*. Wydawnictwa Geologiczne, Warszawa, 37 pp. [In Polish.]

Burtan, J., Sokołowski, S., Sikora, W., Żytko, K., 1959. *Szczegółowa Mapa Geologiczna Polski, arkusz Milówka 1:50 000*. Wydawnictwa Geologiczne, Warszawa. [In Polish.]

Burtanówna, J., Konior, K. & Książkiewicz, M., 1937. *Mapa geologiczna Karpat polskich*. Polska Akademia Umiejętności, Kraków. [In Polish.]

Cieszkowski, M., Golonka, J., Krobicki, M., Ślączka, A., Waśkowska, A. & Wendorff, M., 2009. Olistholits within the Silesian Series and their connections with evolutionary stages of the Silesian Basin. *Geologia*, 35: 13–21. [In Polish, with English summary.]

Cotton, C. A., 1950. Tectonic scarps and fault valleys. *Geological Society of America Bulletin*, 61: 717–758.

Dadlez, R. & Jaroszewski, W., 1994. *Tektonika*. Wydawnictwo PWN, Warszawa, 743 pp. [In Polish.]

Davis, G. H., Reynolds, S. J. & Kluth, C. F., 2011. *Structural Geology of Rocks and Regions, 3rd Edition*. John Wiley and Sons, New York, 839 pp.

Decker, K., Neścieruk, O., Reiter, F., Rubinkiewicz, J., Ryłko, W. & Tokarski, A. K., 1997. Heteroaxial shortening, strike-slip faulting and displacement transfer in the Polish Carpathians. *Przegląd Geologiczny*, 45: 1070–1071.

Doktór, S., Graniczny, M. & Pożaryski, W., 1988. The main photolineaments of Poland and the surrounding areas and their connection with geology. *Biuletyn Instytutu Geologicznego*, 359: 61–70.

Dunne, W. M. & Hancock, P. L., 1994. Paleostress analysis of small scale brittle structures. In: Hancock, P. L. (ed.), *Continental Deformation.* Pergamon Press, Cambridge, pp. 101–120.

Geroch, S. & Nowak, W., 1980. Stratigraphy of the Flysch in the borehole *Łodygowice IG-1* (Western Carpathians, Poland). *Rocznik Polskiego Towarzystwa Geologicznego*, 50: 341–390. [In Polish, with English summary.]

Golonka, J. & Krobicki, M., 2017. The Position of the West Carpathians in the Alpine-Carpathian Fold-And-Thrust Belt. In: Krobicki, M. (ed.), *Abstract Volume & Field Trip Guidebook. 6th International Symposium of the International Geoscience Programme (IGCP) Project-589. Development of the Asian Tethyan Realm: Genesis, Process and Outcomes. Western Tethys meets Eastern Tethys, Kraków (Poland), 29 September – 5 October 2017.* Polish Geological Institute – National Research Institute, Warsaw, pp. 63–65.

Golonka, J., Waśkowska, A. & Ślączka, A., 2019. The Western Outer Carpathians: Origin and evolution. *Zeitschrift der Deutschen Gesellschaft für Geowissenschaften,* 170: 229–254.

Grabowski, D., Marciniec, P., Mrozek, T., Neścieruk, P., Rączkowski, W., Wójcik, A. & Zimnal, Z., 2008. *Instrukcja opracowania Mapy osuwisk i terenów zagrożonych ruchami masowymi w skali 1:10 000*. Państwowy Instytut Geologiczny, Warszawa, 92 pp. [In Polish.]

Graniczny, M., 1989. Fotolineamenty i ich znaczenie geologiczne. *Instrukcje i Metody Badań Geologicznych Państwowego Instytutu Geologicznegoh*, 50: 1–72. [In Polish.]

Graniczny, M., 1994. Strefy nieciągłości tektonicznych w świetle korelacji wielotematycznych danych geologicznych, na przykładzie Żarnowca i Ziemi Kłodzkiej. *Instrukcje i Metody Badań Geologicznych Państwowego Instytutu Geologicznego*, 54: 1–82. [In Polish.]

Graniczny, M. & Mizerski, W., 2003. Lineaments in the satellite imagery of Poland – an attempt of recapitulation. *Przegląd Geologiczny*, 51: 474–482. [In Polish, with English summary.]

Hancock, P. L., 1985. Brittle microtectonics: principles and practice. *Journal of Structural Geology*, 7: 437–457.

Hennings, P. H., Olson, J. E. & Thompson, L. B., 2000. Combining outcrop data and three-dimensional structural models to characterize fractured reservoirs: an example from Wyoming. *AAPG Bulletin*, 84: 830–849.

Hobbs, W. H., 1904. Lineaments of the Atlantic Border Region. *Geological Society of America Bulletin*, 1: 483–506.

Hobbs, W. H., 1912. *Earth Features and Their Meaning*. McMillan Co., New York, 506 pp.

Jankowski, L. & Margielewski, W., 2014. Structural control on the Outer Carpathians relief: a new approach. *Przegląd Geologiczny*, 62: 29–35. [In Polish, with English summary.]

Jankowski, L. & Margielewski, W., 2022. Geological control of young orogenic mountain morphology: From geomorphological analysis to reinterpretation of geology of the Outer Western Carpathians. *Geomorphology*, 386: 107749.

Jaroszewski, W., 1972. Mesoscopic structural criteria of tectonics of nonorogenic areas: an example from the northeastern Mesozoic margin of the Góry Świętokrzyskie Mountains. *Studia Geologica Polonica*, 38: 1–210. [In Polish, with English summary.]

Jaroszewski, W., 1980. *Tektonika uskoków i fałdów*. Wydawnictwa Geologiczne, Warszawa, 295 pp. [In Polish.]

Jaroszewski, W. & Piątkowska, A., 1988. On the nature of some lineaments (exemplified by the Roztocze Ridge, SE Poland). *Annales Societalis Geologorum Poloniae*, 58: 423–443. [In Polish, with English summary.]

Koçal, A., Duzgun H. S. & Karpuz, C., 2004. Discontinuity mapping with automatic lineament extraction from high resolution satellite imagery. In: Altan, O. (ed.), *Proceedings of the XXth ISPRS Congress*, *Technical Commission VII*, *Istanbul, Turkey, July 12–23 2004*. ISPRS Archives, XXXV Part B7, Istambul, pp. 1073–1078.

Koike, K., Nagano, S. & Ohmi, M., 1995. Lineament analysis of satellite images using a Segment Tracing Algorithm (STA). *Computers and Geosciences*, 21: 1091–1104.

Konon, A., 2001. Tectonics of the Beskid Wyspowy Mountains (Outer Carpathians, Poland). *Geological Quarterly*, 45: 179–204.

Kováč, M., Márton, E., Oszczypko, N., Vojtko, R., Hók, J., Králiková, S., Plašienka, D., Klučiar, T., Hudáčková, N. & Oszczypko-Clowes, M., 2017. Neogene palaeogeography and basin evolution of the Western Carpathians, Northern

Pannonian domain and adjoining areas. *Global and Planetary Change,* 155: 133–154.

Kováč, M., Plašienka, D., Soták, J., Vojtko, R., Oszczypko, N., Less, G., Ćosović, V., Fügenschuh, B. & Králiková, S., 2016. Paleogene palaeogeography and basin evolution of the Western Carpathians, Northern Pannonian domain and adjoining areas. *Global and Planetary Change*, 140: 9–27.

Książkiewicz, M. (ed.), 1953. *Regionalna Geologia Polski, T. 1, Karpaty, Z. 2, Tektonika*. Polskie Towarzystwo Geologiczne, Kraków, pp. 362–422. [In Polish.]

Książkiewicz, M., 1968. Observations on jointing in the Flysch Carpathians. *Rocznik Polskiego Towarzystwa Geologicznego*, 38: 335–384. [In Polish, with English summary.]

Książkiewicz, M., 1972. *Budowa Geologiczna Polski, Tom 4, Tektonika, Część 3, Karpaty*. Wydawnictwa Geologiczne, Warszawa, 228 pp. [In Polish.]

Liszkowski, J. & Stochlak, J., 1976. *Szczelinowatość masywów skalnych*. Wydawnictwa Geologiczne, Warszawa, 312 pp. [In Polish.]

Ludwiniak, M., 2008. Joint-network evolution in the western part of Podhale Flysch (Inner Carpathians, Poland). *Przegląd Geologiczny*, 56: 1092–1099. [In Polish, with English summary.]

Mah, A., Taylor, G. R., Lennox, P. & Balia, L., 1995. Lineament Analysis of Landsat Thematic Mapper Images, Northern Territory, Australia. *Photogrammetric Engineering and Remote Sensing*, 61: 761–773.

Margielewski, W., 2002. Geological control on the rocky landslides in the Polish Flysch Carpathians. *Folia Quaternaria*, 73: 53–68.

Margielewski, W., 2006. Structural control and types of movements of rock mass in anisotropic rocks: Case studies in the polish Flysch Carpathians. *Geomorphology*, 77: 47–68.

Margielewski, W., Szura, C. & Urban, J., 2008. *Jaskinia Miecharska cave (Beskid Śląski Mts., Outer Carpathians) – The largest non-karst cave in the Flysch Carpathians. Zacisk: Biuletyn KTJ "Speleoklub" Bielsko-Biała*, 2008, pp. 7–13.

Margielewski, W., Urban J. & Szura, C., 2007. Jaskinia Miecharska cave case study of a crevice-type cave developed on a sliding surface. *Nature Conservation*, 63: 57–68.

Mastella, L., 1972. Interdependence of joint density and thickness of layers in the Podhale Flysch. *Bulletin de l'Académie Polonaise des Sciences de la Terre*, 20: 187–196.

Mastella, L., 1988. Structure and evolution of Mszana Dolna tectonic window, Outer Carpathians, Poland. *Annales Societatis Geologorum Poloniae*, 58: 53–173. [In Polish, with English summary.]

Mastella, L. & Konon, A., 2001. Tectonic bending of the Outer Carpathians in the light of joints analysis in the Silesian Nappe. *Przegląd Geologiczny*, 50: 541–550. [In Polish, with English summary.]

Mastella, L. & Konon, A., 2002. Jointing in the Silesian Nappe (Outer Carpathians, Poland) – paleostress reconstruction. *Geologica Carpathica*, 53: 315–325.

Mastella, L. & Szynkaruk, E., 1998. Analysis of the fault pattern in selected areas of the Polish Outer Carpathians. *Geological Quarterly*, 42: 263–276.

Mastella, L. & Zuchiewicz, W., 2000. Jointing in the Dukla Nappe (Outer Carpathians, Poland): an attempt at palaeostress reconstruction. *Geological Quarterly*, 44: 377–390.

Mastella, L., Zuchiewicz, W., Tokarski, A. K., Rubinkiewicz, J., Leonowicz, P. & Szczęsny, R., 1997. Application of joint analisys for paleostress reconstruction in structurally complicated settings: case study from Silesian nappe, Outer Carpathians (Poland). *Przegląd Geologiczny*, 45: 1064–1066.

Mierzejewski, M. P., 1992. Spękania. In: Mierzejewski, M. P. (ed.), *Badania elementów tektoniki na potrzeby kartografii wiertniczej i powierzchniowej. Instrukcje i metody badań geologicznych Państwowego Instytutu Geologicznego*, 51, pp. 132–145. [In Polish.]

Nemati, S. F., Hafezi Moghadas, N., Lashkaripour, G. R. & Sadeghi, H., 2021. Identification of hidden faults using determining velocity structure profile by spatial autocorrelation method in the west of Mashhad plain (Northeast of Iran). *Journal of Mountain Science,* 18: 3261–3274.

Neścieruk, P., 2001. *Płaszczowina śląska w dorzeczu Soły – polskie Karpaty Zachodnie*. Unpublished PhD Thesis. Państwowy Instytut Geologiczny, Kraków, 91 pp. [In Polish.]

Neścieruk, P. & Szydło, A., 2003. Pozycja warstw istebniańskich w Beskidzie Morawsko-Śląskim. *Sprawozdania z Posiedzeń Państwowego Instytutu Geologicznego*, 60: 67–68. [In Polish.]

Neścieruk, P. & Wójcik, A., 2012. *Objaśnienia do Szczegółowej Mapy Geologicznej Polski, arkusz Skoczów (1011) 1:50 000 (reambulacja)*. Państwowy Instytut Geologiczny – Państwowy Instytut Badawczy, Warszawa, 52 pp. [In Polish.]

Neścieruk, P. & Wójcik, A., 2013a. *Szczegółowa Mapa Geologiczna Polski, arkusz Skoczów (1011) 1: 50 000 (reambulacja)*. Państwowy Instytut Geologiczny – Państwowy Instytut Badawczy, Warszawa. [In Polish.]

Neścieruk, P. & Wójcik, A., 2013b. *Objaśnienia do Szczegółowej Mapy Geologicznej Polski arkusz Bielsko-Biała (1012) 1: 50 000 (reambulacja)*. Państwowy Instytut Geologiczny – Państwowy Instytut Badawczy, Warszawa, 55 pp. [In Polish.]

Neścieruk, P. & Wójcik, A., 2014. *Szczegółowa Mapa Geologiczna Polski, arkusz Bielsko-Biała (1012) 1:50 000 (reambulacja)*. Państwowy Instytut Geologiczny – Państwowy Instytut Badawczy, Warszawa. [In Polish.]

Neścieruk, P. & Wójcik, A., 2016. *Objaśnienia do Szczegółowej Mapy Geologicznej Polski, arkusz Wisła 1: 50 000 (reambulacja)*. Państwowy Instytut Geologiczny - Państwowy Instytut Badawczy, Warszawa, 33 pp. [In Polish.]

Neścieruk, P. & Wójcik, A., 2017. *Szczegółowa Mapa Geologiczna Polski arkusz Wisła 1: 50 000 (reambulacja)*. Państwowy Instytut Geologiczny – Państwowy Instytut Badawczy, Warszawa. [In Polish.]

Nowak, J., 1927. *Zarys Tektoniki Polski*. II Zjazd Słowiańskich Geografów i Etnografów w Polsce, Kraków, 160 pp. [In Polish.]

O'Leary, D. W, Friedman, J. D. & Pohn, H. A., 1976. Lineament, linear, lineation: Some proposed new standards for old terms. *Geological Society of America Bulletin*, 87: 1463–1469.

Ostaficzuk, S., 1981. Lineaments as representation of tectonic phenomena against a background of some examples from Poland. *Biuletyn Geologiczny Uniwersytetu Warszawskiego*, 29: 195–267. [In Polish, with English summary.]

Oszczypko, N., Ślączka, A. & Żytko, K., 2008. Tectonic subdivision of Poland: Polish Outer Carpathians and their foredeep. *Przegląd Geologiczny*, 56: 927–935. [In Polish, with English summary.]

Ozimkowski, W., 2008. Lineaments of Tatra Mts. surroundings – DEM vs. MSS. *Przegląd Geologiczny*, 56: 1099–1099. [In Polish, with English summary.]

Ozimkowski, W., 2010. Effect of direction of sun shading on geological interpretation of DEM – examples from the Western Carpathians. *Przegląd Geologiczny*, 58: 862–866. [In Polish, with English summary.]

Pánek, T., Margielewski, W., Tábořík, P., Urban, J., Hradecký, J. & Szura, C., 2010. Gravitationally induced caves and other discontinuities detected by 2D electrical resistivity tomography: Case studies from the Polish Flysch Carpathians. *Geomorphology*, 123: 165–180.

Pánek, T., Tábořík, P., Klimeš, J., Komárková, V., Hradecký, J. & Štastný, M., 2011. Deep-seated gravitational slope deformations in the highest parts of the Czech Flysch Carpathians: Evolutionary model based on kinematic analysis, electrical imaging and trenching. *Geomorphology*, 29: 92–112.

Paul, Z., Ryłko, W. & Tomaś, A., 1996. Geological structure of the western part of the Polish Carpathians. *Geological Quarterly*, 40: 501–520.

Pescatore, T. & Ślączka, A., 1984. Evolution models of two flysch basins: the northern Carpathians and the Southern Apennines. *Tectonophysics,* 106: 49–70.

Ragan, D. M., 1973. *Structural Geology: An Introduction to Geometrical Techniques. 2nd Edition*. John Wiley and Sons, New York, 632 pp.

Ramsay, J. G., 1967. *Folding and Fracturing of Rocks*. McGraw-Hill, New York, 568 pp.

Ramsay, J. G. & Huber, M. I., 1987. *The Techniques of Modern Structural Geology, Vol. 2, Folds and Fractures*. Pergamon Press, London, 391 pp.

Rauch, M., 2013. The Oligocene–Miocene tectonic evolution of the northern Outer Carpathian fold-and-thrust belt: insights from compression-and-rotation analogue modelling experiments. *Geological Magazine*, 150: 1062–1084.

Rauch, M., 2015. Formation of chaotic complexes associated with overthrusts, on the basis of analog modelling results. *Nafta-Gaz*, 9: 601–664. [In Polish, with English summary.]

Riedel, W., 1929. Zur Mechanik geologischer Brucherscheinungen. *Zentralblatt für Mineralogie, Geologie und Paläontologie*, 1929B: 354–368.

Rubinkiewicz, J., 1998. Development of joints in Silesian Nappe (Western Bieszczady, Carpathians, SE Poland). *Przegląd Geologiczny*, 46: 820–826. [In Polish, with English summary.]

Rubinkiewicz, J., 2000. Development of fault pattern in the Silesian Nappe: Eastern Outer Carpathians, Poland. *Geological Quarterly*, 44: 391–404.

Rubinkiewicz, J., 2007. Fold-thrust-belt geometry and detailed structural evolution of the Silesian nappe – Eastern part of the Polish Outer Carpathians (Bieszczady Mts.). *Acta Geolologica Polonica,* 57: 479–508.

Rybak, B., 2006. Kinematics indicators from thrust zones in the Polish Outer Carpathians (southern Poland). *Przegląd Geologiczny*, 54: 905–912. [In Polish, with English summary.]

Ryłko, W., 2018. *Szczegółowa Mapa Geologiczna Polski, arkusz Milówka (1029) 1: 50 000 (reambulacja)*. Państwowy Instytut Geologiczny - Państwowy Instytut Badawczy, Warszawa. [In Polish.]

Ryłko, W., 2019. *Objaśnienia do Szczegółowa Mapy Geologicznej Polski arkusz Milówka (1029) 1:50 000 (reambulacja).* Państwowy Instytut Geologiczny – Państwowy Instytut Badawczy, Warszawa, 74 pp. [In Polish.]

Ryłko, W. & Żytko, K., 1980. Kierunki poszukiwań węglowodorów we fliszu Karpat Zachodnich na podstawie dotychczasowych badań. *Przegląd Geologiczny*, 28: 547–552. [In Polish.]

Scheiber, T., Fredin, O., Viola, G., Jarna, A., Gasser, D. & Łapinska-Viola, R., 2015. Manual extraction of bedrock lineaments from high resolution LiDAR data: methodological bias and human perception. *GFF*, 137: 362–372.

Schmid, M. S., Fügenschuh, B., Kounov, A., Matenco, L., Nievergelt, P., Oberhänsli, R., Pleuger, J., Schefer, S., Schuster, R., Tomljenović, B., Ustaszewski, K. & van Hinsbergen, D. J. J., 2020. Tectonic units of the Alpine collision zone between Eastern Alps and western Turkey. *Gondwana Research*, 78: 308–374.

Sikora, R., 2017. Landslides and its relation with faults and hidden fractures zones – results from the LiDAR-based DEM and structural analysis (Silesian Beskid, Outer Carpathians). In: Alonso, E. & Pinyol, N. (eds), *JTC1 2017, First JTC1 Workshop on Advances in Landslide Understanding, 24–26 May 2017, Barcelona.* International Center for Numerical Methods in Engineering (CIMNE), Barcelona, pp. 126–129.

Sikora, R., 2018. Structural control on the initiation and development of the Biała Wisełka Landslide Complex (Silesian Beskid, Outer Carpathians, Southern Poland). *Geology, Geophysics & Environment*, 44: 31–48.

Sikora, R., 2022. Geological and geomorphological conditions of landslide development in the Wisła source area of the Silesian Beskid mountains (Outer Carpathians, southern Poland). *Geological Quarterly*, 66: 19. https://10.7306/gq.1651

Sikora, R. & Piotrowski, A., 2013a. *Mapa osuwisk i terenów zagrożonych ruchami masowymi w skali 1:10 000, gm. Wisła, pow. cieszyński, woj. śląskie.* Państwowy Instytut Geologiczny – Państwowy Instytut Badawczy. [In Polish.] http://mapa.osuwiska.pgi.gov.pl [20/4/2022]

Sikora, R. & Piotrowski, A., 2013b. *Objaśnienia do Mapy osuwisk i terenów zagrożonych ruchami masowymi w skali 1:10 000, gm. Wisła, pow. cieszyński, woj. śląskie.* Państwowy Instytut Geologiczny – Państwowy Instytut Badawczy, Warszawa, 29 pp. [In Polish.] http://mapa.osuwiska.pgi.gov.pl [20/4/2022]

Skempton, A. W., 1966. Some observations on tectonic shear zones. *Proceeding of the 1st International Conference on Rock Mechanisms*. International Society for Rock Mechanics, Lisbon, pp. 329–-335.

Słomka, T., 1995. Deep-marine siliciclastic sedimentation of the Godula Beds, Carpathians. *Prace Geologiczne PAN*, 139: 1–132. [In Polish, with English summary.]

Solon, J., Borzyszkowski, J., Bidłasik, M., Richling, A., Badora, K., Balon, J., Brzezińska-Wójcik, T., Chabudziński, Ł., Dobrowolski, R., Grzegorczyk, I., Jodłowski, M., Kistowski, M., Kot, R., Krąż, P., Lechnio, J., Macias, A., Majchrowska, A., Malinowska, E., Migoń, P., Myga-Piątek, U., Nita, J., Papińska, E., Rodzik, J., Strzyż, M., Terpiłowski, S. & Ziaja, W., 2018. Physico-geographical mesoregions of Poland: Verification and adjustment of boundaries on the basis of contemporary spatial data. *Geographica Polonica*, 2: 143–170.

Strzeboński, P., 2022. Contrasting styles of siliciclastic flysch sedimentation in the Upper Cretaceous of the Silesian Unit, Outer

Western Carpathians: sedimentology and genetic implications. *Annales Societatis Geologorum Poloniae*, 92: 159–180.

Suzen, M. L. & Toprak, V., 1998. Filtering of satellite images in geological lineament analyses: An application to a fault zone in Central Turkey. *International Journal of Remote Sensing*, 19: 1101–1114.

Szajnocha, W., 1923. Przekrój warstw karpackich między Ustroniem a źródłowiskami Wisły pod Magórką i Baranią. *Rocznik Polskiego Towarzystwa Geologicznego*, 1: 1–20. [In Polish.]

Teisseyre, H., 1971. Structural analysis in the Sudetes Mts. *Rocznik Polskiego Towarzystwa Geologicznego*, 41: 93–118. [In Polish, with English summary.]

Tokarski, A. K., 1975. Structural analysis of the Magura unit between Krościenko and Zabrzeż (Polish Flysch Carpathians). *Rocznik Polskiego Towarzystwa Geologicznego*, 45: 327–359.

Tokarski, A. K., Zuchiewicz, W. & Świerczewska, A., 1999. The influence of early joints on structural development of thrust–and-fold belts: A case study from the Outer Carpathians (Poland). *Geologica Carpathica Special Issue*, 50: 178–180.

Tomaszczyk, M., 2005. Correlation between orientation of pseudokarst caves and joints in NE part of the Silesian Beskid Mts. (Outer Carpathians). *Przegląd Geologiczny*, 53: 168–174. [In Polish, with English summary.]

Turner, F. J. & Weiss, L. E., 1963. *Structural Analysis of Metamorphic Tectonites*. McGraw-Hill, New York, 545 pp.

Tusikova, S., Markuloca, T. & Gil'manova, G., 2020. Seismic activity of major hidden faults in the Priamurye region. In: Rasskazov, I. & Tkach, S. (eds), *VIII International Scientific Conference "Problems of Complex Development of Georesources*" *E3S Web of Conferences. Journal of Proceedings,* 192: 04010.

Unrug, R., 1963. Istebna Beds – a fluxoturbidity formation in the Carpathian Flysch. *Rocznik Polskiego Towarzystwa Geologicznego*, 33: 49–92.

Unrug, R., 1980. Tectonic rotation of flysch nappes in the Polish Outer Carpathians. *Rocznik Polskiego Towarzystwa Geologicznego*, 50: 27–39.

Vollmer, F. W., 2015. Orient 3: a new integrated software program for orientation data analysis, kinematic analysis, spherical projections, and schmidt plots. *GSA Annual Meeting in Baltimore*, *Maryland, USA (1–4 November 2015). Geological Society of America Abstracts with Programs,* 47(7): 49.

Wallbrecher, E., 1986. *Tektonische und Gefugeanalytische Arbeitsweisen. Graphische, Rechnerische und Statistische Verfahren*. Enke, Stuttgart, 244 pp.

Watkins, H., Healy, D., Bond, C. & Butler, R., 2018. Implications of heterogeneous fracture distribution on reservoir quality; an analogue from the Torridon Group sandstone, Moine Thrust Belt, NW Scotland. *Journal of Structural Geology*, 108: 180–197.

Weidman, L., Maloney, J. M. & Rockwell, T. K., 2019. Geotechnical data synthesis for GIS-based analysis of fault zone geometry and hazard in an urban environment. *Geosphere*, 15: 1999–2017.

Will, T. M. & Wilson, C. J. L., 1989. Experimental produced slickenside lineations in pyrophyllic clay. *Journal of Structural Geology,* 11: 657–667.

Wojciechowski, T., 2009. *Geologiczna analiza osuwisk z wykorzystaniem satelitarnej interferometrii radarowej na przykładzie rejonu Nowego Sącza*. Unpublished PhD Thesis, Silesian University, Sosnowiec, 133 pp. [In Polish.]

Wójcik, A., 1997. Landslides in the Koszarawa drainage basin – structural and geomorphological control (Western Carpathians, Beskid Żywiecki Mts). *Biuletyn Państwowego Instytutu Geologicznego*, 376: 5–42. [In Polish, with English summary.]

Żaba, J., 1999. The Structural evolution of Lower Palaeozoic Succession in the Upper Silesia Block and Małopolska Block Border Zone (Southern Poland). *Prace Państwowego Instytutu Geologicznego*, 166: 1–166. [In Polish, with English summary.]

Zuchiewicz, W., 1997. Reorientation of the stress field in the Polish Outer Carpathians in the light of joint pattern analysis. *Przegląd Geologiczny*, 45: 105–109. [In Polish, with English summary.]

Zuchiewicz, W., 1999. Morphometric techniques as a tool in neotectonic studies of the Polish Carpathians (southern Poland). *Przegląd Geologiczny*, 47: 851–854. [In Polish, with English summary.]

Zuchiewicz, W., 2001. Geodynamics and neotectonics of the Polish Outer Carpathians (southern Poland). *Przegląd Geologiczny*, 49: 710–716. [In Polish, with English summary.]

Zuchiewicz, W. & Henkiel, A., 1993. Orientation of Late Cainozoic stress field axes in the light of joint pattern analysis in SE part of the Polish Carpathians. *Annales Universitetis M. Curie-Skłodowska*, 48: 311–348. [In Polish, with English summary.]

Zuchiewicz, W. & McCalpin, J. P., 2000. Geometry of faceted spurs on an active normal fault: case study of the Central Wasatch fault, Utah, USA. *Annales Societatis Geologorum Poloniae*, 70: 231–249.

Zuchiewicz, W., Tokarski, A. K., Jarosiński, M. & Márton, E., 2002. Late Miocene to present day structural development of the Polish segment of the Outer Carpathians. *EGU Stephan Mueller Special Publication Series*, 3: 185–202.

Żytko, K., 1999. Symmetrical pattern of the late Alpine features of the northern Carpathian basement, their foreland and hinterland; orogen and craton suture. *Prace Państwowego Instytutu Geologicznego*, 168: 165–194. [In Polish, with English summary]

Żytko, K., Zając, R., Gucik, S., Ryłko, W., Oszczypko, N., Garlicka, I., Nemčok, J., Elias, M., Mencik, E. & Stranik, Z., 1988. *Map of Tectonic Elements of the Western Outer Carpathians and their Foreland*. In: Poprawa, D. & Nemčok, J. (eds), *Geological Atlas of the Western Carpathians and their Foreland*. Państwowy Instytut Geologiczny, Warszawa.